SEARCH FOR SUPERSYMMETRY (SUSY) WITH TOPOLOGICAL VARIABLES AT THE LHC

A THESIS SUBMITTED TO
THE GRADUATE SCHOOL OF NATURAL AND APPLIED SCIENCES
OF
MIDDLE EAST TECHNICAL UNIVERSITY

BY

MESUT ÜNAL

IN PARTIAL FULFILLMENT OF THE REQUIREMENTS
FOR
THE DEGREE OF MASTER OF SCIENCE
IN
PHYSICS

AUGUST 2015

Approval of the thesis:

SEARCH FOR SUPERSYMMETRY (SUSY) WITH TOPOLOGICAL VARIABLES AT THE LHC

submitted by **MESUT ÜNAL** in partial fulfillment of the requirements for the degree of **Master of Science in Physics Department, Middle East Technical University** by,

Prof. Dr. Gülbin Dural Ünver _____
Dean, Graduate School of **Natural and Applied Sciences**

Prof. Dr. Mehmet Tevfik Zeyrek _____
Head of Department, **Physics**

Prof. Dr. Mehmet Tevfik Zeyrek _____
Supervisor, **Physics Department, METU**

Assoc. Prof. Dr. Muammer Altan Çakır _____
Co-supervisor, **Physics Engineering Dept., Istanbul Tech. Uni.**

Examining Committee Members:

Prof. Dr. Meltem Serin
Physics Department, METU _____

Prof. Dr. Mehmet Tevfik Zeyrek
Physics Department, METU _____

Prof. Dr. Altuğ Özpineci
Physics Department, METU _____

Assoc. Prof. Dr. İsmail Turan
Physics Department, METU _____

Prof. Dr. Ali Ulvi Yılmazer
Physics Engineering Department, Ankara University _____

Date: _____

I hereby declare that all information in this document has been obtained and presented in accordance with academic rules and ethical conduct. I also declare that, as required by these rules and conduct, I have fully cited and referenced all material and results that are not original to this work.

Name, Last Name: MESUT ÜNAL

Signature :

ABSTRACT

SEARCH FOR SUPERSYMMETRY (SUSY) WITH TOPOLOGICAL VARIABLES AT THE LHC

Ünal, Mesut

M.S., Department of Physics

Supervisor : Prof. Dr. Mehmet Tevfik Zeyrek

Co-Supervisor : Assoc. Prof. Dr. Muammer Altan Çakır

August 2015, 71 pages

The primary purpose of this thesis is to compare the effects on signal significance of the topological variables, W-stransverse mass (M_{T2}^{W}) and topness, which would be used in Supersymmetry searches in the single lepton channels in the future collider experiments. In this thesis, Stau-coannihilation scenarios were used as signal samples along with the four major background events, $t\bar{t}$+jets, boson+jets, single top+jets, and diboson, of supersymmetric top squark pair production and cascade decays. These brand new topological variables were proposed as an alternative to the classical variables such as M_T and H_T for background elimination due to the mathematically underconstrained nature of both $t\bar{t}$ and signal cascade decays. Since both the signal and the background samples were required to be produced at higher energies than the experiments conducted up to now, simulation programs such as Pythia and Delphes, were used to produce those samples. With the help of pyROOT data analysis framework, the samples are processed according to the kinematical and topological requirements. The results show that by applying a cut on both M_{T2}^{W} and topness variables separately, a significant increase in the statistical significance of the signal was obtained. Moreover, these variables almost gave the same significance results for all the signal scenarios with or without pile-up.

Keywords: High Energy Physics, Standard Model, Supersymmetry, Dark Matter, Stau-coannihilation, Higgs Boson, Stransverse Mass, Topness, LHC, ATLAS, CMS

ÖZ

TOPOLOJİK DEĞİŞKENLER YARDIMIYLA LHC DENEYLERİNDE SÜPERSİMETRİ (SUSY) ARAŞTIRMALARI

Ünal, Mesut
Yüksek Lisans, Fizik Bölümü
Tez Yöneticisi : Prof. Dr. Mehmet Tevfik Zeyrek
Ortak Tez Yöneticisi : Doç. Dr. Muammer Altan Çakır

Ağustos 2015 , 71 sayfa

Bu tezin öncelikli amacı gelecekte yapılacak olan çarpıştırma deneylerindeki tek lepton kanallarında süpersimetri araştırmalarında kullanılabilecek W-stransverse kütle (M_{T2}^{W}) ve topness topolojik değişkenlerinin sinyalin istatistiksel anlamlılığındaki etkilerinin kıyaslanmasıdır. Bu tezde, $t\bar{t}$+jets, boson+jets, single top+jets ve diboson gibi stop çift oluşumu ve kademeli bozunumunun ana arka plan olaylarının yanında Stau ortak yok oluşu seneryaloı sinyal örnekleri olarak kullanılmıştır. $t\bar{t}$ ve sinyal kademeli bozunumlarının yeterli matematiksel kısıtlamaları olmadığından ötürü bu yeni topolojik değişkenler M_T ve H_T gibi klasik değişkenlere alternative olarak önerilmiştir. Sinyal ve arka plan olaylarının daha önceki deneylerin ulaşamadığı enerjilerde üretilmesi gerektiği için Pythia ve Delphes gibi simülasyon programları bu olayları üretmek için kullanılmıştır. Bu örnekler pyROOT veri analiz sistemi ile kinematik ve topolojik gerekliliklere göre işlenmiştir. Sonuçlar göstermektedir ki, M_{T2}^{W} ve topness değişkenlerinin ikisine birden ayrı ayrı uygulanan kesintiler, sinyalin istatistiksel anlamlılığında kayda değer artışlar sağladı. Ayrıca bu iki topolojik değişken, sinyalin istatistiksel anlamlılığında yığıntı vakalı ve vakasız bütün sinyal senaryoları için neredeyse aynı sonuçları vermiştir.

Anahtar Kelimeler: Yüksek Enerji Fiziği, Standart Model, Süpersimetri, Karanlık

Madde, Stau ortak yok oluşu, Higgs Bozonu, Stransverse Kütle, Topness, LHC, ATLAS, CMS

To my sun and my family

ACKNOWLEDGMENTS

First of all, I would like to show my gratitude to my supervisor, Prof. Dr. Mehmet T. Zeyrek and co-supervisor, Assoc. Prof. Dr. Altan Çakır for their guidance and patience they showed me in my education and research. I couldn‘t have finished my research and this thesis without their guidance.

I would like to express my gratitude to my colleagues and friends, Gökçenur Yeşilyurt, Buğra Bilin, Dr. Sezen Sekmen, and Dr. Efe Yazgan. Without their support on my thesis and their friendship, I could not improve my academic skills that much and could not overcome the obstacles of the challenging nature of the high energy physics community.

I would like to thank my friends Cenk Türkoğlu, Özenç Güngör, Botan Elveren, Dilek Kızılören, Altuğ Elpe, Soner Albayrak, Ozan Dernek, and Gamze Sökmen who helped me to overcome the stressful times in my master‘s education. We shared more things than the times for a lunch.

Special thanks to my sun, other half, and companion to eternity, Güneş Biliciler Ünal for helping me to reason this life. Without her, it would be even harder to find my way in the academic life.

Last but not least, I would like to thank to my family who made me who I am and helped me to make my dreams real. Though they were not by my side in my undergraduate and master‘s education periods, they always believed in me, supported my choices, and helped me to overcome difficulties of my life. They have done all they could do for me without the slightest hesitation.

TABLE OF CONTENTS

LIST OF TABLES

TABLES

LIST OF FIGURES

FIGURES

LIST OF ABBREVIATIONS

ATLAS	A Toroidal LHC ApparatuS
BR	Branching ratio
CMS	Compact Muon Solenoid
DM	Dark Matter
DY	Drell-Yan
EWSB	ElectroWeak Symmetry Breaking
HL-LHC	High Luminosity LHC
GUT	Grand Unification Scale
LHC	Large Hadron Collider
LHCb	Large Hadron Collider beauty
SSB	Spontaneous Symmetry Breaking
SM	Standard Model
STC	Stau-coannihilation
SUSY	Supersymmetry
WIMP	Weakly Interacting Massive Particle

CHAPTER 1

INTRODUCTION

Particle physicists try to find a way out from the constraints of the current valid laws that govern the microcosms of particles. Standard Model (SM) has been valid for almost half a century and gives good predictions for the experimental results. Although the conducted experiments up to now support its claims, SM is not believed to be a fundamental theory and not flawless.

Supersymmetry (SUSY) is one of the most popular and most promising cures for the deficiencies SM has and the troubles SM creates. So far, in the experiments, no sign of SUSY has been observed. Previous experiments set limitations and excluded discovery regions for the further researches. Especially the Run I phase of the Large Hadron Collider (LHC) upset the ones in the favor of SUSY. Yet, Run II phase of the LHC instill hope for us. For the higher collision energies, it is more likely to find heavy SUSY particles. At that point, since such high collision energies have never been experienced so far, it is important to decide which methods should be used in order to identify SUSY signals. Because there will be more pile-up and background rates in the higher energies, it would be a big challenge for the researchers to discriminate signal from the background.

In this research, two brand new variables, which are called stransverse mass and topness, are used for background elimination process. After the classical cuts that are described as control cuts, these two variables are used interchangeably. By comparing their signal significance results, we try to show their efficiencies in the background elimination.

In Chapter 2, a brief theoretical background of the Standard Model and Supersymmetry, which is necessary to understand this thesis, is given. By explaining the flaws of SM, the consequences of the new Higgs boson discovery, and the importance of SUSY, the motivation of the research is evaluated. In Chapter 3, phenomenological meanings of the dedicated topological variables are explained in detail to prepare us for the Analysis part, Chapter 4. In Chapter 4, from analysis tools to analysis results, all aspects of our research are given along with the some necessary concepts such as statistical significance and pile-up.

CHAPTER 2

THEORY

2.1 Standard Model

Standard Model (SM) is a mathematically consistent theory of the strong, electromagnetic, and weak interactions. It explains the most of the relations between the fundamental forces of the universe and the elementary particles. A theory must be Lorentz and gauge invariant to become physical, and surely SM provides it. Its various aspects have been tested successfully with different experiments so far. Despite its fundamental troubles and dilemmas that will be described later in this chapter in more detail, SM come through all the examinations within the scope of its predictions. As described in [1], it is an approximately correct description of nature in the order of the scale $1/1000^{th}$ the size of the atomic nucleus.

The July 4^{th}, 2012 discovery of the scalar Higgs boson, once more, verify the operativeness of SM, because its measured features has showed that the newly discovered scalar has the same behavior with the Higgs boson described in SM. The couplings of the Higgs boson have been probed to measure how much it deviates from the SM predictions in the experiments conducted up to now. Yet, no significant deviation is found according to the latest results [2].

In addition to the previous predictions of SM such as the existence and the features of vector bosons, the charm quark, and the neutral current, very rare decays of the strange B meson (B_s^0) and the B^0 meson into two oppositely charged muons ($\mu^+\mu^-$) are observed just as the same rate SM predicts. SM foresees that for every billion produced B_s^0 mesons four of them decay into $\mu^+\mu^-$, and for every ten billions pro-

duced B^0 mesons one of them decay into $\mu^+\mu^-$ pair [3]. In 2014, both CMS and LHCb experiments, with the data collected in the first run of LHC, announced that they observed these decays just like the SM posits [4]. Combined statistical significances obtained by both CMS and LHCb results are 6σ for $B_s^0 \to \mu^+\mu^-$, and 3σ for $B^0 \to \mu^+\mu^-$ [4].

Though the existence of such results are in favours of SM, it is not considered as a fundamental theory. It has incomplete parts, important problems, and too much arbitrariness to become a complete and a fundamental theory.

First of all, the minimal version of the SM has 20 free parameters for neutrinos with zero mass and 7 additional free parameters for massive Dirac neutrinos. Also, these 7 parameters become 9 if neutrinos are Majorana neutrinos [1].

Second, SM has a gauge symmetry problem. It is a product of $SU(3)\times SU(2)\times U(1)$, but only the SU(2) part is chiral, and unfortunately the reason is unknown. Charge quantization, which is another aspect of gauge symmetry problem, is the other open question. In other words, why all particles have charges multiples of e/3 is unknown [1].

Moreover, fermions have known 3 families, and there is no answer for why there are 3 families instead of 2 or 4. Considering the fact that the known matter only consists of the 1^{st} family, existence of the other families becomes an even harder question. In addition, mass values of the particles of a family are bigger than the masses of the particles of previous families. SM does not predict such a mass hierarchy between the families.

Furthermore, one of the biggest problems of SM is called "gauge hierarchy problem", or "Higgs hierarchy problem" or simply "hierarchy problem". In the presence of a cut-off scale, Λ, which represents the physical energy scale and can be considered as ultraviolet cut-off if there is no any higher scale, Higgs mass is affected by quantum loop corrections. The bare mass (tree-level) of Higgs receives quadratically divergent corrections from loop diagrams as the ones shown in Figure 2.1, and so the measured Higgs mass is written as

$$M_H^2 = (M_H^2)_{bare} + \mathcal{O}(\lambda, g^2, h^2)\Lambda^2 \tag{2.1}$$

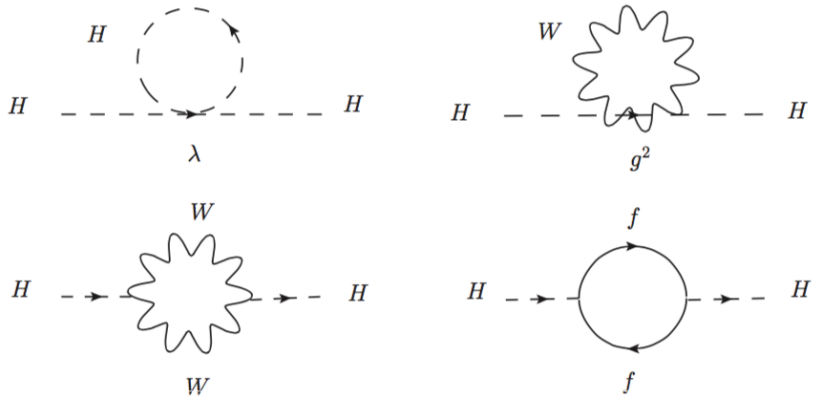

Figure 2.1: Diagrams of various radiative corrections to Higgs mass that are Higgs self-interaction, interactions with gauge bosons, and interactions with fermions.

where λ is the self-coupling parameter, g is the gauge coupling constant, and f is the fermion coupling constant. Such contributions make Higgs mass around cut-off scale. However, due to the Electroweak Symmetry Breaking (EWSB) and the unitarity of WW scattering, Higgs mass must be smaller than 700 GeV [1, 5, 6], and this is the reason of why it is called hierarchy problem. To adjust the theoretical Higgs mass to the experimental value a "fine-tuning" is required, but it makes the theory "unnatural", and it causes the naturalness problem.

Last but not least, SM lacks important ingredients: A sufficient mechanism to explain the existence of dark energy and dark matter. Dark energy contributes to the 74% of the energy density of the Universe, and is responsible for the accelerated expansion of the Universe. On the contrary, dark matter is the "brake" of this expansion. It forms 24% of the energy density of the Universe, and interact with the ordinary matter, which forms the 4-5% of the Universe, attractively to decrease the acceleration of the expansion [7]. However, the common opinion is that dark matter consists of Weakly Interacting Massive Particles (WIMPs) since we cannot directly observe and measure its effect on ordinary matter [8, 9]. Yet, unfortunately, SM does not have a mechanism to help us understand the existence and behavior of both Dark Energy and Dark Matter.

2.2 Beyond the Standard Model and Minimal Supersymmetric Standard Model

Besides the vector gauge bosons, i.e. photons, W and Z bosons, and gluons, SM predicts the existence of an additional scalar boson, Higgs boson, which was described very briefly in the previous section. This scalar boson is the fundamental particle of the Higgs field, and causes the Higgs mechanism. Higgs mechanism is thought to be the reason behind the Electroweak Symmetry Breaking (EWSB), which explains the existence of the massive gauge bosons.

EWSB is simply the breaking of $SU(2) \times U(1)$ symmetry group into U(1) symmetry group. This symmetry breaking happens spontaneously and called Spontaneous Symmetry Breaking (SSB). SSB is formulated by Weinberg and Salam [10, 11], in 1967, after the important achievement of Glashow that is the unification of electromagnetic and weak interactions [12]. Bhattacharyya says in reference [6], "Whenever a system does not show all the symmetries by which it is governed, we say that the symmetry is 'spontaneously' broken. More explicitly, when there is a solution which does not exhibit a given symmetry which is encoded and respected in the Lagrangian, or Hamiltonian, or the equations of motion, the symmetry is said to be spontaneously broken". Without any symmetry breaking, the particle universe is described by the symmetry group, $G = SU(3) \times SU(2) \times U(1)$. This configuration describes a picture that all the gauge bosons are massless. In other words, the system is symmetric in terms of mass. However, the electroweak part of the SM, i.e. $SU(2) \times U(1)$ symmetry group, is spontaneously broken. Before the SSB, the number of total degrees of freedom of the electroweak part is 12, which consists of one complex doublet with four degrees of freedom, one massless gauge boson with two degrees of freedom, and three another massless gauge bosons with six degrees of freedom. After SSB, three of the four degrees of freedom of the complex doublet are eaten by the last three massless gauge bosons. The total number of degrees of freedom is the same, but the constituents are different. These are a massless photon with two degrees of freedom, a scalar Higgs boson with one degrees of freedom, and massive $W^{\pm}$ and Z^0 bosons with nine degrees of freedom from now on. In other words, we can say that three components of the Higgs doublet are eaten by the W and Z bosons, and they gain mass by the Higgs mechanism [13]. On the contrary, gluons do not couple to Higgs and

stay as massless bosons. In Figure 2.2, the famous Mexican hat potential is shown. At $\phi_1 = \phi_2 = 0$, which are the mass eigenstates of the complex doublet, potential takes its maximum value, and the system is symmetric. Yet, when the symmetry is spontaneously broken, potential takes a random value at the circle of $\phi_1 = \phi_2 \neq 0$ that is placed in the bottom of the Mexican hat.

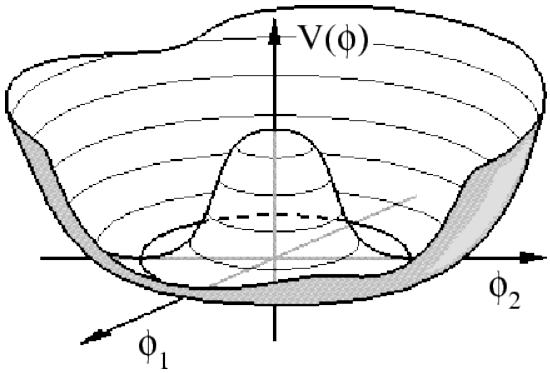

Figure 2.2: Representation of SSB in the shape of Mexican hat potential. Here ϕ_1 and $\phi_2 = 0$ are the mass eigenstates of the complex scalar. For $\phi_1 = \phi_2 = 0$ potential takes its local maximum value along with the symmetry preservation. For $\phi_1 = \phi_2 \neq 0$, symmetry is spontaneously broken, potential drops to the bottom circle of the Mexican hat, and so the gauge bosons require their masses. The figure is taken from [14].

The idea behind the SSB is that while creating the masses of gauge bosons, calculability of the theory is saved. In other words, as it was proved by t'Hooft, SSB does not eliminate the renormalizability of the theory [15, 16]. However, SSB causes Higgs mass to increase enormously. A point like Higgs boson under the Higgs mechanism receives quadratically divergent quantum loop corrections to its mass. As stated in the previous section, there is a theoretical upper limit for Higgs mass around 700 GeV under the assumption of the perturbative weak interaction. So, Higgs mass should be of the order of 10^2 GeV whereas the grand unification scale can be taken as 10^{15} GeV. Grand Unification Theories (GUTs) are used for the unification of the three forces, i.e. electromagnetic, weak, and strong forces, of the Universe except the gravity, and usual limit predicted by the SUSY calculations is 10^{15} GeV as can be seen in Figure 2.3. In this case, one-loop corrections to the Higgs mass become 24 orders of magnitude bigger than the bare mass of Higgs boson. To keep the theory renormalized, bare mass must be fine-tuned to 24 digits [17]. Unless fine-tuning is applied, Higgs

mass becomes closer to the unification scale which is much bigger than the expected upper limit. However, this time, naturalness problem occurs.

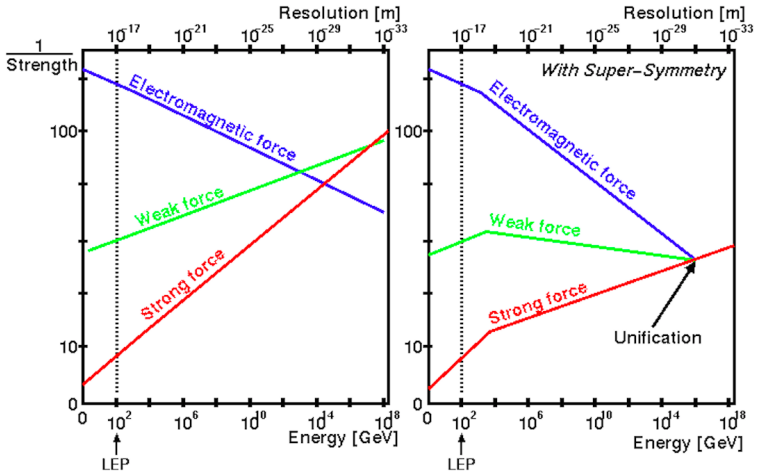

Figure 2.3: Behaviors of the inverse coupling constants with respect to the energy scale. As it can be seen at the left, fundamental forces cannot unite anywhere in SM unlike SUSY scenarios that unites these forces around 10^{15} GeV. The figure is taken from [18].

To solve the abovementioned problems of SM, a new space-time symmetry, supersymmetry or simply SUSY, is developed by Gervais and Sakita [19], Golfand and Likhtman [20], and Volkov and Akulov [21] independently in the beginning of 1970s. It is an extension of the SM's symmetry structure and a renormalizable field theory that interchanges bosons and fermions. According to SUSY, all SM particles have their supersymmetric partners that have not been discovered yet. Moreover, up to the Planck scale, $M_{Pl} \sim 10^{19}$ GeV, all gauge couplings remain perturbative [5]. The SUSY partners of particles have different spins. For instance, SUSY partner of a fermion, quark or lepton, is a spin-0 scalar particle, squarks or sleptons respectively, and SUSY partner of a gauge boson is a spin-1/2 gaugino. Instead of one Higgs doublet as in SM, SUSY proposes two Higgs doublets and their spin-1/2 partners, Higgsinos. Gauginos and Higgsinos mix together to form Dirac charginos with two mass eigenstates ($\tilde{\chi}_r^{\pm}$, $r = 1, 2$), and Majorana neutralinos with four mass eigenstates ($\tilde{\chi}_r^0$, $r = 1...4$). In Figure 2.4, particles and their corresponding SUSY partners are shown.

In 1977, Pierre Fayet posited the first realistic SUSY model, which is called Minimal

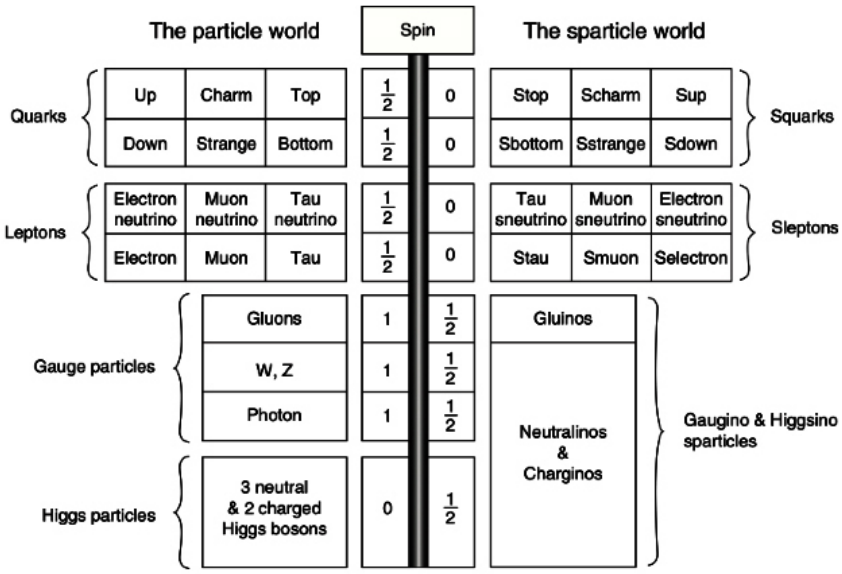

Figure 2.4: SM particles (left) and their SUSY partners (right).

Supersymmetric Standard Model (MSSM) [22]. It is the simplest supersymmetric extension of the SM as is evident from its name. In MSSM, squarks and sleptons are coupled to two SM fermions. Yet, such an interaction violates lepton number and baryon number conservations in addition to the unobserved and unexpected immediate proton decay [5]. To get rid of these problems, a new quantum number is postulated, and it is called R-parity. SM particles are even under the R-parity transformation while SUSY partners are odd under this transformation. In other words, $R = +1$ is assigned for SM particles while $R = -1$ is assigned for their SUSY partners. Then, possible SUSY 3-point gauge interaction vertices are $\tilde{q}\tilde{q}g$, $q\tilde{q}\tilde{g}$, and $\tilde{g}\tilde{g}g$. It means that SUSY particles are always produced in pairs. The vertices with three quarks are not allowed since it leads to rapid proton decay [5].

MSSM, by postulating the intrinsic boson-fermion symmetry, solves the hierarchy problem. The new SUSY partners of the SM particles cancel quadratic divergences and restores naturalness. For instance, the top quark contribution whose diagram is seen in Figure 2.5 (top diagram) to the Higgs mass radiative corrections is

$$(\Delta M_H^2)_t \sim -\frac{N_c (h_t)^2}{4\pi^2}\Lambda^2 \tag{2.2}$$

where $N_c = 3$, which represents the top quark colors, and $h_t = m_t v$, the top-Yukawa coupling with v is the vacuum expectation value [1]. Now, assume that we have two complex scalar fields, ϕ_r where $r = 1, 2$. Their diagrams are the bottom left and the bottom right ones in Figure 2.5, and their contribution to Higgs mass can be written as

$$(\Delta M_H^2)_{\phi_r} \sim \frac{\lambda_r N_c}{8\pi^2}\Lambda^2 \tag{2.3}$$

where λ_r are the coupling constants for each complex scalar [1]. These quadratic divergences cancel each other by $\lambda_1 = \lambda_2 = (h_t)^2$. In the perspective of SM, this can be done by externally. However, fortunately, it is done by supersymmetry automatically. As a result, it can be deduced that these complex scalar fields are the scalar partners of the top quarks, t_L and t_R [1].

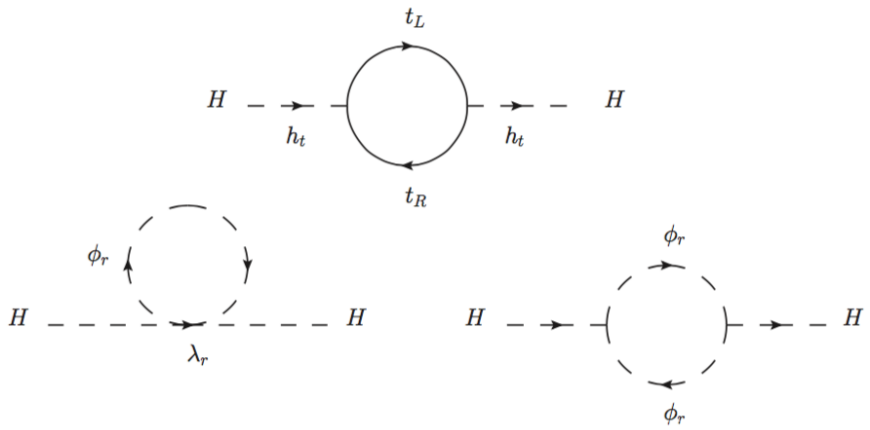

Figure 2.5: Top quark and ϕ_r contributions to M_H^2.

In addition to the solution of the mass hierarchy method, supersymmetry offers several candidates for DM as well. In the R-parity conserving scenarios, lightest supersymmetric particle, LSP, is the DM candidate of SUSY. Since LSP is in R-odd state, it cannot decay into two SM particles. Moreover, as it is the lightest SUSY particle, it cannot decay into another SUSY particles as well. So, it has to be a stable particle and so, a strong candidate for DM. There are three options for LSP; neutralino, sneutrino, and gravitino, which is the SUSY partner of the hypothetical graviton. The LHC friendly version of the MSSM is the phenomenological MSSM (pMSSM). Apart from being measurable, it decreases the number of MSSM constraints. It is

important, because MSSM increases the number of parameters of SM to more than 100 parameters. pMSSM decreases them to 19, and proposes that lightest neutralino ($\tilde{\chi}_1^0$) is the best candidate for DM, because experimental results ruled out the sneutrino possibility. Besides, gravitino couples to other particles gravitationally and as long as it is not LSP, we can rule it out, too [5].

SUSY posits that the SM particles should have the same mass with their SUSY partners; however, no such particles are observed so far, and obviously, this prevents SUSY to become the exact symmetry of the Universe. The reason is that SUSY must be also broken spontaneously. There are two main mechanisms for such a symmetry breaking [17].

First one is the SSB of SUSY. It is a more desirable way than the second possibility that is explained below. However, for such a case, even though symmetry of the Lagrangian is preserved, ground state does not have symmetry. As a result, symmetry in the spectrum of the states is destroyed.

Second, since the first way is not a viable case, breaking the symmetry explicitly by adding terms to the Lagrangian is preferred instead. These terms must be non-invariant under SUSY transformation, and the cancellation of the quadratic divergences must be preserved. Since these terms do not spoil the cancelation of quadratic divergences, this breaking mechanism is called 'explicit SUSY breaking' or 'soft breaking'. In this case, two mass gaining mechanism occur for SUSY particles: The one from the EWSB and the other one from the soft breaking. Even though soft breaking does not disturb the cancellation of the quadratic divergences of the Higgs mass, it leaves a logarithmic dependence for Higgs mass in terms of top mass and the averages of the stop masses, i.e.

$$(m_h^2) \simeq M_Z^2 cos^2(2\beta) + \frac{3m_t^4}{2\pi^2 v^2} ln(\frac{m_{\tilde{t}}^2}{m_t^2}) \tag{2.4}$$

In this equation, $m_{\tilde{t}} = \sqrt{m_{\tilde{t}_1} m_{\tilde{t}_2}}$ and $tan\beta = v_u/v_d$ where v_u and v_d are the vacuum expectation values of up type and down type fermions respectively [6, 23, 24]. Soft breaking requires that $m_{\tilde{t}} > m_t$, so that fine-tuning is inevitable. Unfortunately, this leads to the problem so called "little hierarchy problem", but it is off-topic for

experimentalists for now. As a result, we can deduce that it is wise to search in the region that top squark mass is much bigger that top mass. In the Figure 2.6, neutralino mass vs. stop mass is shown. In the corresponding limit, for this thesis, we work on the rightmost region of this this figure, and assume the existence of on-shell $\tilde{t} \rightarrow t\tilde{\chi}_1^0$ decay.

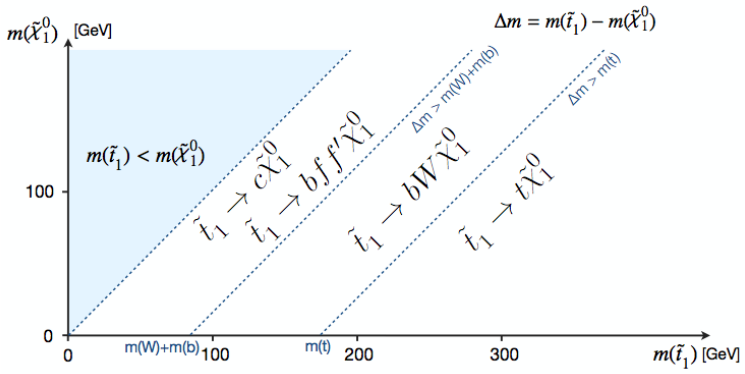

Figure 2.6: Neutralino mass vs. stop mass plane, and region-by-region stop decay possibilities. The figure is taken from [25].

2.3 Importance of the 2012 Higgs discovery and the Motivation of this research

2012 discovery of Higgs boson, which is announced at July 4^{th}, 2012 [26, 27], has opened a new era for particle physics. Higgs was one of the most important missing parts of particles physics, and the discovery caused some theories such as Higgless models and the theories considering Higgs as a composite particle to be ruled out.

What we can deduce from equation 2.4 is that

$$(m_h)^2 = M_Z^2 \cos(2\beta) + \text{radiative corrections} < 135GeV \tag{2.5}$$

[5, 28]. Here, 135 GeV is phenomenological upper limit for the Higgs mass. Luckily, the precision measurements after 2012 Higgs discovery have shown that Higgs mass is approximately $125.09 \pm 0.21(\text{stat.}) \pm 0.11(\text{syst.})$ GeV, which is the combined result of ATLAS and CMS experiments [29]. In Table 2.1, significances of the latest observations results are shown for the most important Higgs decay channels.

Significance ($m_H = 125.0GeV$)		
Combination	**Expected**	**Observed**
H→ZZ	6.3σ	6.5σ
H→ $\gamma\gamma$	5.3σ	5.6σ
H→WW	5.4σ	4.7σ
H→ $\tau\tau$	3.9σ	3.8σ
H→bb	2.6σ	2.0σ
H→ $\mu\mu$	<0.1σ	0.4σ

Table 2.1: Significance results of the CMS experiment for the most important decay modes with integrated luminosities of up to 5.1 fb^{-1} at 7 TeV and up to 19.7 fb^{-1} at 8 TeV, assuming $m_H = 125.0GeV$ [30]. Here expected significance is the median significance of signal hypotheses with a given measurement, and is obtained after the fit of the signal-plus-background hypothesis to the data.

Although these are the desperate times for SUSY searchers since no SUSY particles have been observed so far and the newly discovered Higgs boson shows SM like specifications, as it can be seen in equation 2.5, this Higgs boson is still likely to be the lightest Higgs boson candidate of SUSY. In the perspective of MSSM, three of the eight degrees of freedom of two complex Higgs doublet are eaten by W and Z bosons, five degrees of freedom remain. These remaining degrees of freedom form five physical Higgs fields, which are two scalar Higgs fields (H_1^0, H_2^0), one pseudo-scalar Higgs field (A^0), and a pair of charged Higgs fields ($H^{\pm}$). The scalar states, H_1^0 and H_2^0, mix to mass eigenstates, h^0 and H^0. This h^0 is the so-called lightest Higgs of SUSY. It is a scalar and in the mass range as SUSY proposed, so that it can be said that there is still hope for SUSY [31].

In addition, this research is focused on the single lepton channel, which gives us the possibility to use several types of variables that uses invariant mass concept such as transverse mass and stransverse mass that are explained in next chapter in more detail. Moreover, in addition to single lepton, there should be at least six jets two of which are tagged as b-jets and missing energy. By looking at the jet multiplicity and missing energy distributions, we can eliminate the background even more. First and foremost, after all the classical cuts that used in general SUSY searches, new variables like stransverse mass and topness is used in this research. These are brand new variables and used in previous analysis very few. By comparing their possible effects on signal significance in the future SUSY searches like the ones in 14 TeV LHC or HL-LHC

makes our research even more exciting.

CHAPTER 3

PHENOMENOLOGY OF TOPOLOGICAL VARIABLES FOR SUSY SEARCHES

In this chapter, phenomenological backgrounds of the fundamental variables that are used for this research are explained. The first one, transverse mass or simply M_T, is used in all variations of the cut-list possibilities listed in Chapter 4. As explained below, to a certain extent, it can be effective to discriminate background events from the signal events.

In the later sections of this chapter, more complex variables such as M_{T2}^W and topness are explained in detail. These variables are important for the underconstrained events that cannot be reconstructed properly enough with M_T. Effects of M_{T2}^W and topness variables on signal significance are the main subjects of these thesis, and the comparison of their effects are examined in Chapter 4. To understand the role they would play in the SUSY searches, we need to understand the idea behind them, first.

3.1 Transverse Mass, M_T

Transverse mass, M_T, is a variable that helps us to constrain the mother particle mass that decays into one visible and one invisible particles. Measured transverse momentum, p_T of the visible particle equals to the transverse momentum of the invisible particle. For instance, W boson mass can be determined from the $W \rightarrow l\nu$ decay with the measured p_T of the visible lepton. Here, under the assumption that on-shell W boson decays into lepton and neutrino, M_T is defined as

$$M_T^2 = m_l^2 + m_v^2 + 2(E_T^l E_T^{miss} - \vec{p}_T^{\,l} \cdot \vec{\not{p}}_T) \tag{3.1}$$

where E_T^l and E_T^{miss} are the transverse energies of the lepton and the associated neutrino, and p_T^l and $\not{p}_T$ are the transverse momenta for the lepton and missing energy, respectively. The beam direction is chosen to be along z-axis so that $\vec{p}_T^{\,l} = (\vec{p}_x, \vec{p}_y)$. Then,

$$E_T^l = \sqrt{m_l^2 + |\vec{p}_T^{\,l}|^2} \tag{3.2}$$

$$E_T^{miss} = \sqrt{m_v^2 + |\vec{\not{p}}_T|^2} \tag{3.3}$$

If m_l and m_v are negligibly small, equation 3.1 can be written as

$$M_T^2 = 2(E_T^l E_T^{miss} - \vec{p}_T^{\,l} \cdot \vec{\not{p}}_T) \tag{3.4}$$

and

$$M_T^2 = 2E_T^l E_T^{miss}(1 - cos\phi) \tag{3.5}$$

where $(E_T^{miss})^2 = \vec{\not{p}}_T^{\,2}$ and ϕ is the angle between the lepton and the neutrino in azimuthal plane with respect to the incoming beam direction as stated in [32]. As a result, it constraints the W mass, which means M_T endpoint gives the m_W, i.e.

$$M_T^2 \leq m_W^2 \tag{3.6}$$

that holds only when the rapidity of the l and ν are equal to each other [33].

3.2 Stransverse Mass, M_{T2}

M_{T2} variable, which is also called stransverse mass, is a topological variable that is closely related to M_T variable. It was first introduced by C. G. Lester and D. J. Summers [34] to overcome the calculation difficulties for the mother particle mass of the cascade decades that includes more than one missing particles.

As stated in the Section 3.1, M_T is a common and useful variable to determine the W mass via the transverse momenta of lepton and missing neutrino. Yet, in a hadron collider, the parity odd particles are produced in pairs, and the result is a cascade decay ending at stable particles [35]. In MSSM theory, which requires the R-parity, the lightest parity-odd particle is a stable dark matter candidate, i.e. Lightest Supersymmetric Particle (LSP). Since it is a weakly interacting particle, it is impossible to be detected. In both branches of cascade decays, LSPs are created along with the neutrinos. In addition to the missing particles problem, total momentum in the beam direction cannot be measured, and it is even more difficult to determine the mother particle mass [35]. Some kinematical variables such as $\not{p}_T$ and E_T can give estimations for the new particle masses, but they are sensitive to mass differences of new particles and model dependent. So, it is not viable to test the trueness of a new theory, since determining the particle masses is the first step to confirm a new theory. Hence, instead of model dependent approaches, model independent approaches are approved. In such approaches, invariant mass distributions are used. By looking at the endpoints of the distributions whose positions are functions of the particles involved in the decay one can determine the requested masses. Yet, it requires long decay chains and thus a lot of constraints. It is impossible to apply these techniques to analyse the short decay chains.

For short decay chains, two main approaches are used. First one is based on kinematic constraints such as constraints resulted from $\not{p}_T$ measurements and the mass-shell constraints. It is assumed that the event topology is known and all the intermediate particles are on shell. Apart from such techniques that are solely depends on 4-momenta, M_{T2} variable, which is defined only on the plane transverse to the beam direction, is a clever way for mass determination as concluded in [35]. In the R-parity conserving scenario, primary particle is pair produced and both of them decay into

undetected LSPs, and the event kinematics is left underconstrained. In the aforementioned cascade decay, we expect a similar decay process for both of the branches of the decay.

For a typical SUSY event resulting to production of sleptons ($\tilde{l}$), the decay process can be shown as

$$pp \rightarrow X + \tilde{l}_R^+ \tilde{l}_R^- \tag{3.7}$$

and

$$\tilde{l}^+ \tilde{l}^- \rightarrow l^+ l^- \tilde{\chi}_1^0 \tilde{\chi}_1^0 \tag{3.8}$$

It seems that the mother particle mass in this decay can be calculated via M_T, but since we have massive undetected particle, chargino, we have to use M_{T2}. For equation 3.8, we can write,

$$m_{\tilde{l}}^2 = m_l^2 + m_{\tilde{\chi}}^2 + 2(E_{Tl}E_{T\tilde{\chi}}cosh(\Delta\eta) - \vec{p}_{Tl} \cdot \vec{p}_{T\tilde{\chi}}) \tag{3.9}$$

where $E_T = \sqrt{\vec{p_T^2} + m^2}$ and $(\Delta\eta)$ is the rapidity between l and $\tilde{\chi}$. For $cosh(\Delta\eta) \geq 1$, i.e. $\Delta\eta \geq 0$,

$$m_{\tilde{l}}^2 \geq m_T^2(\vec{p}_{Tl}, \vec{p}_{T\tilde{\chi}}) \equiv m_l^2 + m_{\tilde{\chi}}^2 + 2(E_{Tl}E_{T\tilde{\chi}} - \vec{p}_{Tl} \cdot \vec{p}_{T\tilde{\chi}}) \tag{3.10}$$

Although we cannot measure the missing transverse momenta of neutrino and neutralino separately, the total missing transverse momenta can be measured and be written as

$$\vec{\not{p}}_T = \vec{p}_{T\chi_a} + \vec{p}_{T\chi_b} \tag{3.11}$$

where a and b are arbitrary indices describing the neutralinos. Hence, equation 3.10 becomes

$$m_{\tilde{l}}^2 \geq max\{m_T^2(\vec{p}_{Tl-}, \vec{p}_{T\tilde{\chi}_a}), m_T^2(\vec{p}_{Tl+}, \vec{p}_{T\tilde{\chi}_b})\} \tag{3.12}$$

Yet, since we don′t know which neutralino is a or b, it is wisely advised in [34] to write equation 3.10 as

$$m_{\tilde{l}}^2 \geq M_{T2}^2 \equiv \min_{\vec{\not{p}}_1+\vec{\not{p}}_2=\vec{\not{p}}_T} [max\{m_T^2(\vec{p}_{Tl^-}, \vec{\not{p}}_1), m_T^2(\vec{p}_{Tl^-}, \vec{\not{p}}_2)\}] \tag{3.13}$$

where the neutralino mass is a free parameter. In equation 3.13, the larger M_T value is chosen since either of the M_T values cannot exceed the parent particle mass if the true momenta are used. The minimization on trial neutralino momenta fulfilling the E_T^{miss} constraint is used to avoid obtaining a M_{T2} value that exceeds the mother particle mass [36]. In other words, if the assumed daughter particles′ masses are equal or less than the true masses, M_{T2} is bounded from above by the mother particle mass. Thus, we can define M_{T2} as the minimal mother particle mass compatible with the postulated event topology and an assumed daughter particle mass [35]. The distribution of M_{T2} has an endpoint at the primary particle mass. If the assumed neutralino mass is less (more) than its true mass value, the endpoint will be below (above) the true mother particle mass.

3.3 W-Stransverse Mass, M_{T2}^W

Even though more than three variations of M_{T2} are listed in [37] such as M_{T2}^b and M_{T2}^{bl}, M_{T2}^W is the most suitable one, among others, especially for single lepton background with two intermediate on-shell W bosons, which one of them decays into an observed lepton and a neutrino. M_{T2}^W can be defined as the minimal mother particle mass that can be compatible with the all transverse momentum and mass-shell constraints of the event topology [37]. Here, the superscript W is for the on-shell W boson information. For this variable, mass of the mother particle, i.e. top quark, is not explicitly used, but implicitly bounded by the event. The difference between the original M_{T2} and M_{T2}^W is that we use all the mass-shell constraints of the cascade decay for M_{T2}^W calculations, and instead of taking the maximum of two sides of M_T,

unlike the original M_{T2}, it is directly defined as the minimisation in consideration of mass shell conditions. The relation of the M_{T2}^W in terms of event kinematics is seen in equation 3.14, and the event topology of the single lepton background originated from dileptonic $t\bar{t}$ decay can be seen in Figure 3.1.

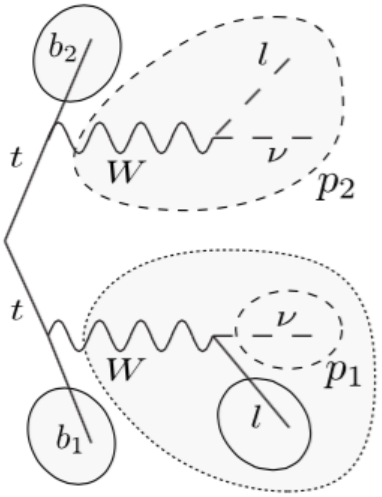

Figure 3.1: Event topology of the dileptonic $t\bar{t}$ cascade decay with labels for M_{T2}^W variable. Here p_2 is the entire missing momentum, and p_1 is just for the missing neutrino of the observed lepton. The figure is taken from [37].

$$M_{T2}^W = min\left\{ m_y \text{ consistent with: } \left[\begin{array}{r} \vec{p}_1^{\,T} + \vec{p}_2^{\,T} = \vec{E}_T^{miss}, p_1^2 = 0, (p_1 + p_l)^2 = p_2^2 = M_W^2, \\ (p_1 + p_l + p_{b_1})^2 = (p_2 + p_{b_2})^2 = m_y^2 \end{array} \right] \right\} \tag{3.14}$$

where $\vec{E}_T^{miss} = \vec{\not{p}}_T$.

3.4 Topness

Topness is an alternative variable to M_{T2}^W for the elimination of the $t\bar{t}$ background. It is first proposed by Michael L. Graesser and Jessie Shelton in 2013 [38]. Its purpose is the suppression of the dominant backgrounds such as dileptonic top decay described in section 4.4, like M_{T2}^W. As described in [38], topness is effective for all signal searches whose main background is dileptonic tops with one missing lepton. However, its efficiency is higher for stop pair production with asymmetric final state,

$\tilde{t}\tilde{t}^* \rightarrow t\tilde{\chi}_1^0\bar{b}\tilde{\chi}_1^0 + h.c.$, which is examined in section 4.2 in more detail.

As stated in previous sections, when one of the leptons of the dileptonic background is lost, one of the mass shell conditions is lost as well. Thus, the system becomes underconstrained, and the variables like M_T are no longer works efficiently enough to discriminate background in a proper way. Instead, missing mass-shell condition is replaced with the minimization of reconstructed center-of-mass energy of the event. At this point, a function S is defined as a measure of how well an event can be reconstructed pursuant to the dileptonic top pair hypothesis for the minimum value of S. S is defined as

$$S(p_{W_x}, p_{W_y}, p_{W_z}, p_{l_z}) = \frac{(m_W^2 - p_W^2)^2}{a_W^4} + \frac{(m_t^2 - (p_{b_1} + p_l + p_l)^2)^2}{a_t^4} + \frac{(m_t^2 - (p_{b_2} + p_W)^2)^2}{a_t^4} + \frac{(4m_t^2 - (\sum_i p_i)^2)^2}{a_{CM}^4} \quad (3.15)$$

where $a_W = 5$GeV, $a_t = 15$GeV, and $a_{CM} = 1$TeV along with the mass-shell conditions, $p_l^2 = 0$, $p_W^2 = m_W^2$, and transverse momentum conservation relations. Finally, topness is defined as

$$t = ln(minS) \quad (3.16)$$

[38]. Since the calculation of the minimization of S is a non-trivial problem, iterations methods are preferable to calculate it.

CHAPTER 4

ANALYSIS

In this chapter, the results of the analysis are explained in addition to the analysis tools and the topologies of the both background and signal processes. After explaining the required knowledge for the analysis, a cut-flow, which is a list of applied cuts in an order, is listed. This step-by-step examination of the background elimination process shows us how we can eliminate the background, and obtain the signal events effectively, i.e. to which points the cuts should be applied in order not the eliminate signal events along with the background events as much as possible.

Inclusive search part of the analysis contains the common variables that are applied in almost all the SUSY searches. For instance, missing transverse energy, $\Delta\phi$, H_T, and missing transverse mass cuts, which are explained in more detail in this chapter, are applied repectively. As described below, a hard cut on such distributions eliminate an important amount of the backgrounds. Yet, for the underconstrained events, they might eliminate the good events as well. Thus, this affects our results negatively, and we need more appropriate variables to increase the signal significance, which quantifies the probability of the existence of the wanted events.

In the last part of this chapter, M_{T2}^W and topness variables are applied for this purpose. These variables serve at almost the same purpose, and used interchangeably. First, M_{T2}^W is applied just after the cut-flow that includes the above-mentioned variables. Then instead of M_{T2}^W, topness is applied, and the significance results of them are compared, because the aim of this research is to compare the effects of these two variables on signal significance in the single lepton, multi jet, and missing energy channel.

4.1 Analysis Tools

The signal scenarios that are used in this research are based on the predictions at 14 TeV collision energies. Since we have no real data obtained with a real detector at these energies, some simulations programs are used to estimate the events. The calculations of the signal scenarios, which is explained in section 4.3, are done with SOFTSUSY 3.4.0 [39] in combination with the SUSY-HIT 1.3b/3.4 [40]. These models are based on SUSY Les Houches Accord, which is a standard for SUSY predictions taken by SUSY authorities in Les Houches meetings. The type of such files are called SLHA files, i.e. end with ".slha", and processed with MADGRAPH 5 [41, 42]. The output of this process is the Les Houches Events (LHE). Then, to obtain fragmentation and hadronization of the events, these LHE files are run through PYTHIA 6.4 [43]. In addition, DELPHES 3.0.10 [44], which is also called "fast simulation", is used for detector simulation for all kind of detectors.

Pythia is a software that is used to generate events with multiparticle productions in collisions. Within the perspective of our understandings on particle physics, it can produce events that would be emerged as a result of electron-positron, pp or ep collisions [43]. The produced realistic events are the inputs of detector simulations.

For the phenomenological studies, instead of using complex detector features, fast detector simulations, which use simplified approaches, are preferred. Delphes 3 is the preferred one in our research. It contains almost all the detector features such as a track propagation system embedded in a magnetic field, electromagnetic and hadron calorimeters, and a muon identification system [44]. So, jets, isolated electrons, muons and photons, taus, and missing energy, can be reconstructed realistically enough for the purposes like ours. Apart from the features of previous versions, Delphes 3 has particle-flow algorithm whose aim is to identify the resulting particles of a collision by combining the information of the different subdetectors optimally [45] and is (was) widely used by the CMS (ALEPH) experiments especially in Run I phase of the LHC. However, as I said, it is not a full detector simulation and lacks some complexities of real detectors such as fake rate of electron, muon, and photon misidentification. Yet, it still works good enough for general purpose detector simulations. It has also pile-up simulation and mitigation features that will be important

for the next phases of the LHC as well as our study. Moreover, it has the flexibility to use it in electron-positron collider simulations along with hadron collisions [44]. In this research Snowmass specified Delphes data cards are used for both signal and background simulations [46].

Finally, these Pythia and Delphes simulated data cards are analysed with pyROOT program. ROOT is a data analysis framework based on C++ language. It was designed at CERN and used in various experiments then. The "py" in front of the ROOT refers to extended version of the ROOT. By extending it in such a way, ROOT can be compatible with the Python features and allow us to use Python scripts with it. Our ROOT macros give us the flexibility to assign various cuts, to tag specific particles, and to plot the necessary figures.

4.2 Topology of the Single Lepton Channel

Single lepton channel is one of the most promising channels for SUSY searches and used in this research. To achieve the cancellation of large loop corrections to the Higgs boson mass, the most viable scenarios among others requires stop and gluino masses below approximately 500 GeV and 1.5 TeV, respectively. According to this scenario top squark is the lightest quark partner, and it leads to multiple W boson, multiple b quarks and two LSPs in final state in the perspective of R-parity conservation [47].

This thesis focuses on the final state that contains single-lepton, multiple jets, at least two of which are b-tagged jets and two LSPs, which are undetected and taken into account as missing energy along with the neutrino that is coupled to our one and only detected lepton. These final state particles are originated from either directly produced top squark pair or gluino associated top squark pair. For both cases, different number of jets is expected such as at least four jets for direct stop production and at least six jets for gluino associated stop production. We know that BR of $\tilde{t} \rightarrow t \rightarrow Wb$ decay is 100 % [48], so we are 100 % sure that at least two b jets are produced. In Figures 4.1 and 4.2, Feynman diagrams of direct top squark production and gluino associated top squark productions are shown, respectively. In Figures 4.3, Feynman

diagrams of leptonic top decay is represented. For $\bar{t}$ decay, diagram is the same except the charge conjugate of the daughter particles are produced.

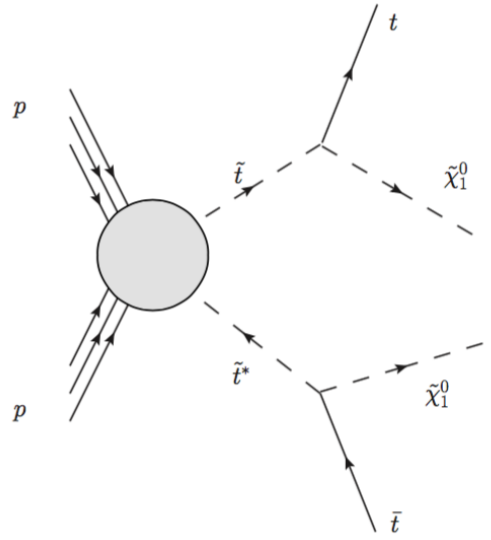

Figure 4.1: Event topology of the direct top squark production and top squark decay

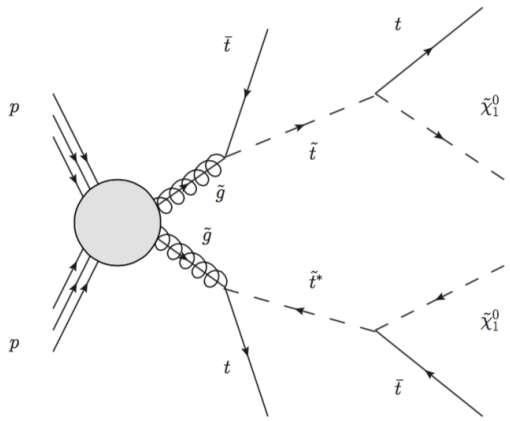

Figure 4.2: Event topology of the gluino associated top squark production and top squark decay

In addition to top squark decay into neutralino and top quark subprocess, top squark also can decay into b quark and chargino pairs that lead to neutralino and W boson final state again. In Figure 4.4, the Feynman diagram of this process is shown. In Figure 4.5, besides symmetric decay processes mentioned above, an asymmetric decay channel is shown. It is like the mixture of the processes in Figure 4.1 and Figure 4.4. Again, the final state is the same, but only the subprocesses are different asymmetrically. Hermitian conjugate of either of its branches is also possible.

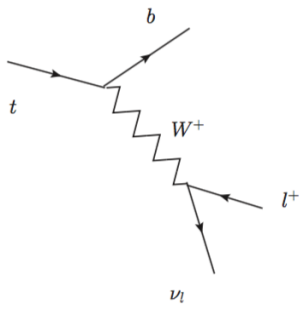

Figure 4.3: Event topology of the leptonic top quark decay

In the previous SUSY searches done by the LHC experiments, simplified SUSY models were used. In simplified SUSY, only on-shell SUSY pair productions are taken into account, and the branching fraction of the specified decay channel is assumed to be 100%. On the contrary, we used non-simplified models that have variety of top squark decay modes. While some these decay modes are presented in this section, rest of them are explained in section 4.4.

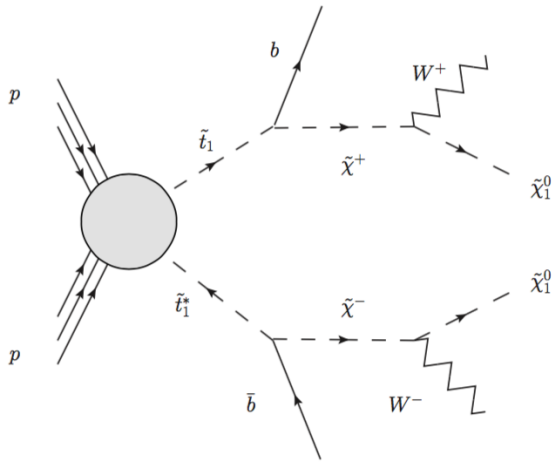

Figure 4.4: Event topology of the direct top squark production and top squark decay with different subprocesses

Single lepton channel, which is sometimes called the golden channel has a very important role for SUSY searches, because gluino associated stop pair production with one of the four W bosons decays leptonically has a probability of approximately 40% [47], and direct stop production with two of the W bosons decay leptonically has a probability of approximately 44% [49] and 30% for e and μ only.

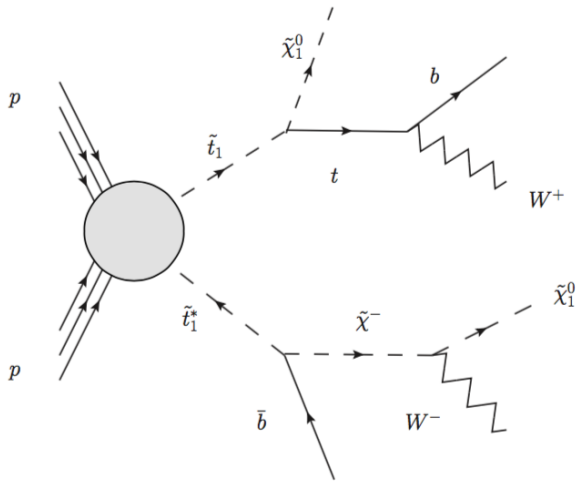

Figure 4.5: Event topology of an asymmetric top squark pair decay. It leads to the same final situation with the previous symmetric processes.

As it is declared in previous chapters, we have not observed any SUSY signal up to now. In Figure 4.6, distributions of M_T, E_T^{miss}, and M_{T2}^W, which were obtained by CMS detector in the $\sqrt{s} = 8$ TeV collisions, are shown [50]. In Figure 4.7, distributions of E_T^{miss} and topness, which were obtained by ATLAS detector in the $\sqrt{s} = 8$ TeV collisions, are shown [25]. For both analysis results, it can be said that significance of the signal points is far from the discovery band. To see a signal above the 5σ, obviously, we need more data and higher collision energies.

4.3 Signal Samples (Stau Coannihilations)

Lightest neutralino, (as stated before), i.e. LSP, is the Dark Matter candidate of the R-parity conserving MSSM, and is a linear combination of the SUSY partners of the neutral gauge and Higgs bosons. Thermal relic scenario is thought to be the explanation for the origin of the dark matter. According to original thermal relic scenario, at the early times of the universe, DM particles were in equilibrium with the surrounding cosmic bath with the help of frequent interactions. Yet, the expansion and cooling of the universe caused Boltzmann suppressed interaction rate to be dropped under the rate of the expansion of the universe and so the equilibrium has been disturbed. As a

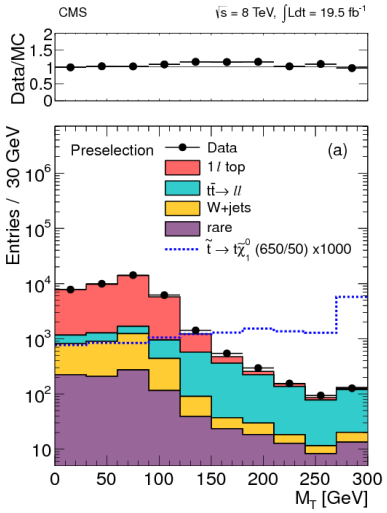

(a) M_T distribution at 8 TeV

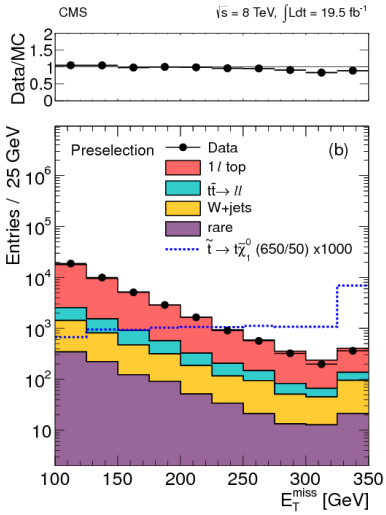

(b) E_T^{miss} distribution at 8 TeV

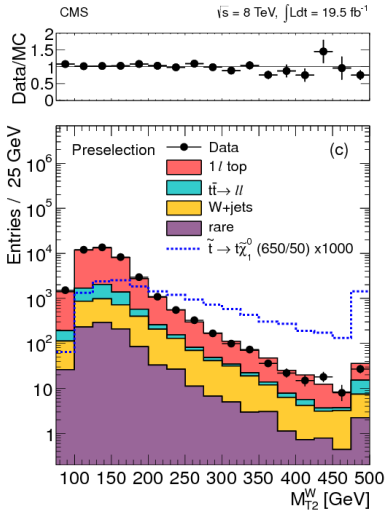

(c) M_{T2}^W distribution at 8 TeV

Figure 4.6: M_T, E_T^{miss}, and M_{T2}^W results of CMS experiment at 8 TeV collision energy. The figures are taken from [50].

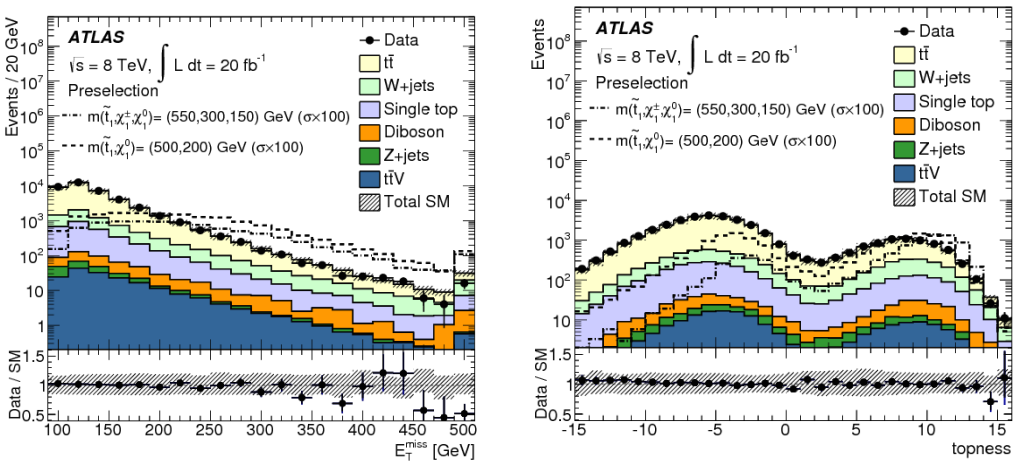

(a) E_T^{miss} distribution at 8 TeV

(b) Topness distribution at 8 TeV

Figure 4.7: E_T^{miss} and topness results of ATLAS experiment at 8 TeV collision energy. The figures are taken from [25].

result, the so-called particle freeze-out started, and the particle number density started to redshift due to the annihilation processes [51]. However, not only the annihilation models of $\tilde{\chi}_1^0$, as pointed out in [52], but also the coannihilations with other supersymmetric particles heavier than the neutralino should be taken into account since the original thermal relic scenario, $\tilde{\chi}_1^0$ annihilation, is not enough to explain the DM abundance. The current observationally bounded value of the relic density is

$$\Omega_{DM}h^2 \propto m_{DM}xn_{DM} \gtrsim 0.11 \tag{4.1}$$

[53]. Stau-$\tilde{\chi}_1^0$ coannihilation, or just Stau Coannihilation (STC) is one of the common ways for the prediction of the Dark Matter relic density calculations. STC lies in the parameter space that is in agreement with the pre-LHC results with the highest likelihood [54]. In this allowed parameter space region, mass difference of stau-NLSP and $\tilde{\chi}_1^0$-LSP ($\Delta M = m_{stau} - m_{\tilde{\chi}_1^0}$) is taken in the range of 5-15 GeV. Thanks to this small choice of mass range, coannihilation can be valid for the early universe, and DM relic density can reach its current abundance [55].

To be more specific, in this thesis, stau and $\tilde{\chi}_1^0$ masses nearly degenerate; $m_{stau} = 194$ GeV and $m_{\tilde{\chi}_1^0} = 187$ GeV [46]. If this mass degeneracy between stau and $\tilde{\chi}_1^0$ is

observed in LHC, it would be highly possible that $\tilde{\chi}_1^0$ was the dark matter.

In this research, four main signal benchmark points have been used; STC4, STC5, STC6 and STC8. Since the total SUSY cross section at LHC mainly depends on the lightest stop mass, for these four scenarios only $\tilde{t}_1$ mass changes from 293 GeV to 735 GeV respectively. While the production cross section of the top squark decreases significantly, production cross section of the electroweak particles stays almost same. Mass spectrums of the benchmark points are shown in Figures 4.8, 4.9, 4.10, and 4.11, and the cross section values of each for different center-of-mass collision energies can be seen in Figure 4.12.

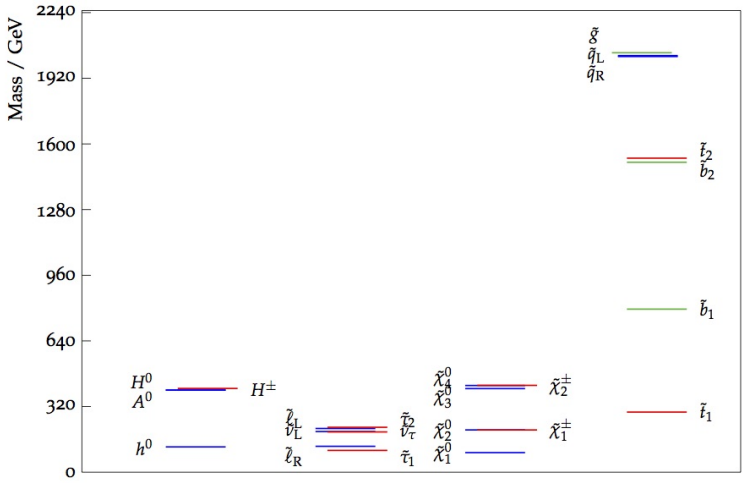

Figure 4.8: The mass spectrum of STC4 with $m_{\tilde{t}_1} = 293.1$ GeV. The figure is taken from [56].

4.4 Backgrounds

The main SM backgrounds for this research are $t\bar{t}$+jets, boson(W or Z)+jets, single top production with additional jets, and diboson. Other possible backgrounds are $t\bar{t}Z$, $t\bar{t}H$, and Drell-Yan(DY)+jets production, but their contributions are too small and suppressed by jet multiplicity requirements. In the figures 4.13, 4.14, 4.15, and 4.16, Feynman diagrams of the background processes are shown.

In this research, we used two possible background uncertainty values; 15% and 20%. These assumptions are based on the research done at 8 TeV collisions energies by

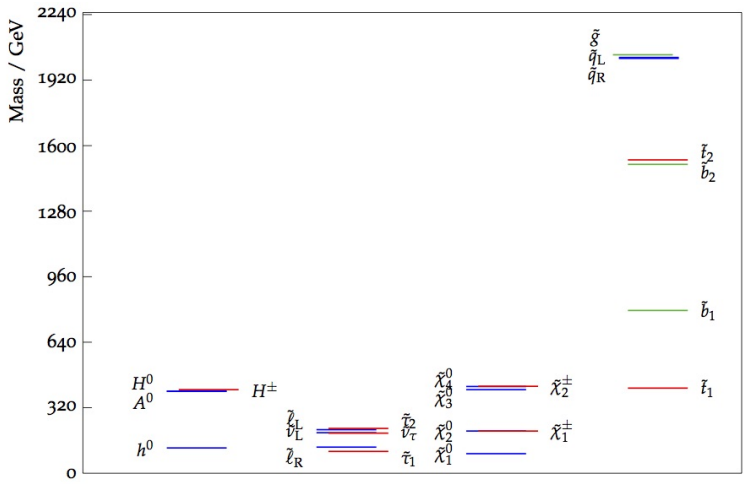

Figure 4.9: The mass spectrum of STC5 with $m_{\tilde{t}_1} = 415.7$ GeV. The figure is taken from [56].

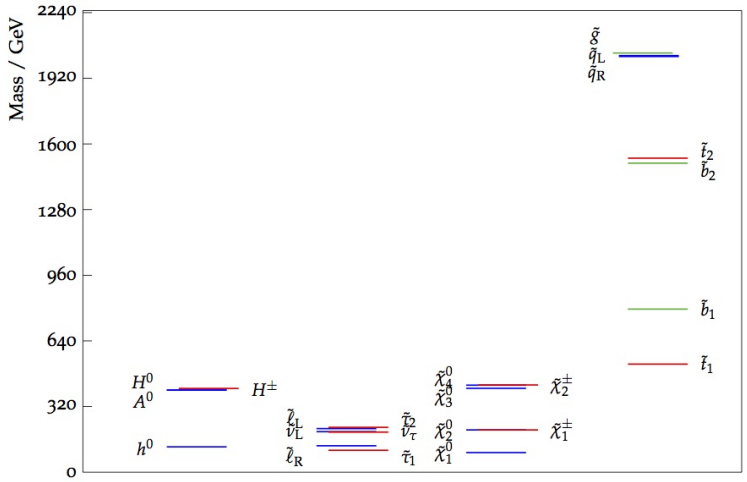

Figure 4.10: The mass spectrum of STC6 with $m_{\tilde{t}_1} = 526.9$ GeV. The figure is taken from [56].

CMS experiment [50]. In [50], it can be seen that measured systematical background uncertainties vary from 15% to 25%, so that it is applicable for us to use such values.

In addition to the SM backgrounds, there exist SUSY backgrounds as well. Unlike simplified SUSY models that top squarks only decay into $t\tilde{\chi}_1^0$ or $b\tilde{\chi}_1^0$, we use non-simplified models in this thesis that include a variety of other top squark decay possibilities. For instance, in our STC models, only 4% of $\tilde{t}_1\tilde{t}_1^*$ events decay into $(t\tilde{\chi}_1^0)(t\tilde{\chi}_1^0)$. Moreover, bottom squark pair production is a considerable process that leads to the production of $b\tilde{\chi}_1^0$ and $t\tilde{\chi}_1^\pm$ events. In Section 4.7, the necessary cuts are

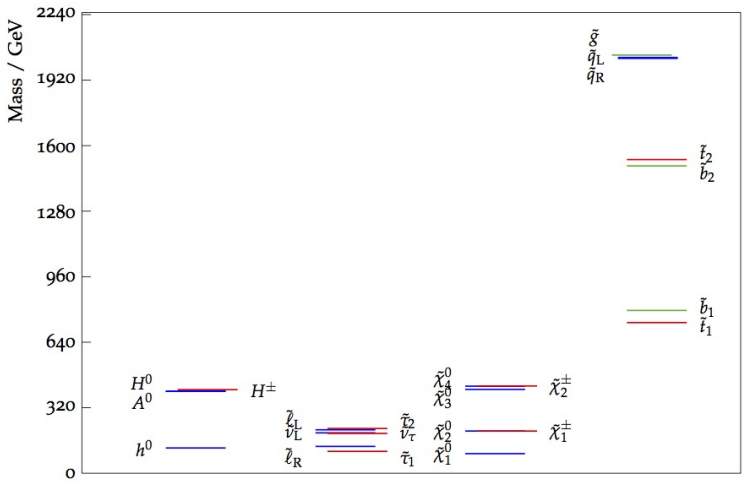

Figure 4.11: The mass spectrum of STC8 with $m_{\tilde{t}_1} = 735.7$ GeV. The figure is taken from [56].

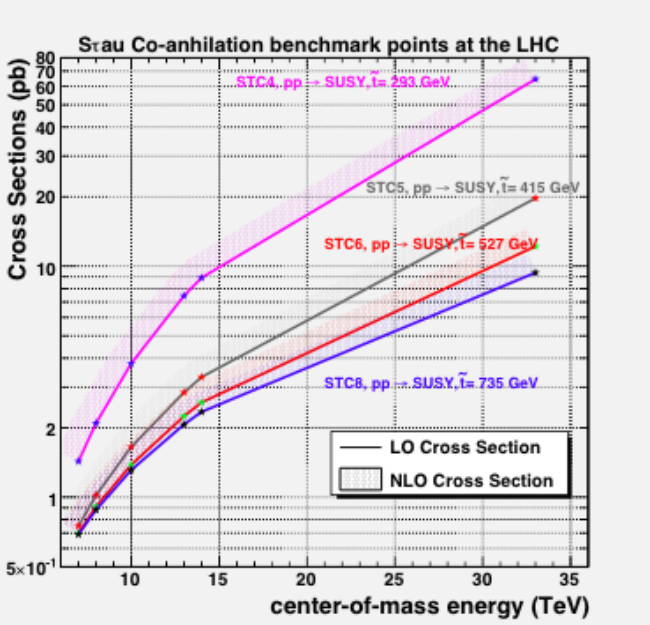

Figure 4.12: Cross sections of four benchmark points for various collision energies. The figure is taken from [46].

listed to eliminate these backgrounds.

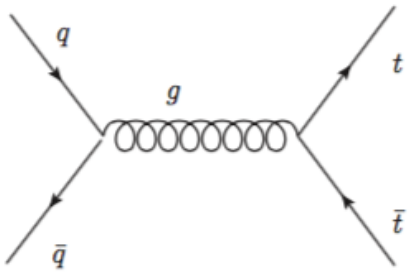

Figure 4.13: Event topology of the $t\bar{t}$+jets background

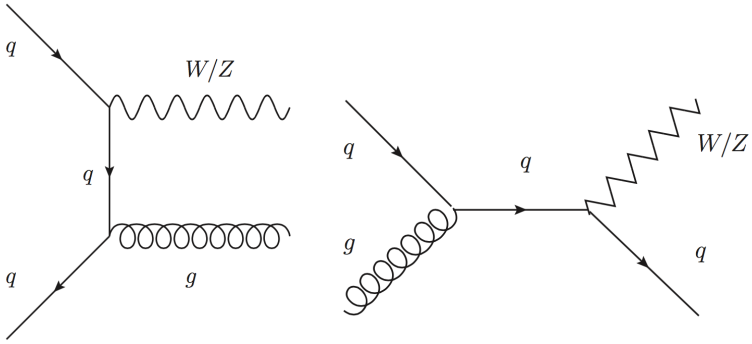

(a) Gluon jet (b) Quark jet

Figure 4.14: Event topologies of the boson(W or Z)+jets backgrounds

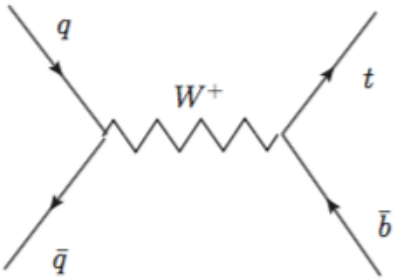

Figure 4.15: Event topology of the single top+jets background

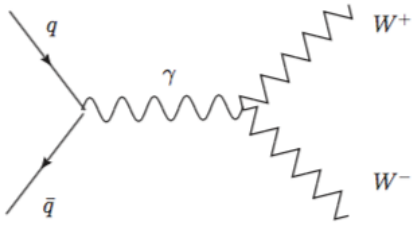

Figure 4.16: Event topology of the diboson background

4.5 Pile-up Events

Besides background events, pile-up events are the other important challenge for the analysis of high luminosity collisions. It is simply defined as the secondary proton-proton collisions overlapping the primary interactions or the number of collisions per bunch crossing. Considering the fact that higher luminosity values will be reached in colliders, especially after the start of Run-II phase of LHC, it is compulsory to take pile-up events into account for this research as well.

In the Run-II of LHC, integrated luminosity will reach to 300 fb^{-1} and approximately 50 pile-up events or more are expected per bunch crossing [57, 46]. Also in this research, two more pile-up cases are analyzed; no pile-up and 140 pile-up. 140 pile-up events are for even higher luminosities such as 3000 fb^{-1} [46, 58, 59, 60]. Thus, to predict the results of future HL-LHC plans with 33 TeV, we carry out an analysis for 140 pile-up cases, too. The case of no pile-up events seems optimistic, but important for us to compare the validity of our results.

4.6 Statistical Significance of Signal

Statistical significance of a signal scenario is a mathematical quantity that is used for inspecting whether there is a discovery or not in a research. To establish a discovery, one should reject the background only hypothesis, i.e. null hypothesis.

First of all, this null hypothesis is assumed to be the true scenario. In, other words, SM background is true, and there is no new physics according to this hypothesis for our case. Thus, the deviation from null hypothesis describes how much we are close to a discovery. This deviation is quantified as σ. For a discovery, it is required that our signal events distribution deviates from background only hypothesis with at least 5σ, whereas the hint for a new physics requires at least 3σ. 3σ means that the reason for the deviation is the statistical fluctuations of background with a possibility of 0.27%, i.e. there is a 0.27% possibility that background only hypothesis is true. Likewise, 5σ means that there is a 0.000057% possibility that background only hypothesis is true. In Figure 4.17, a Gaussian distribution with the points that corresponds to some

specific standard deviation values, and the percentile values for these points can be seen.

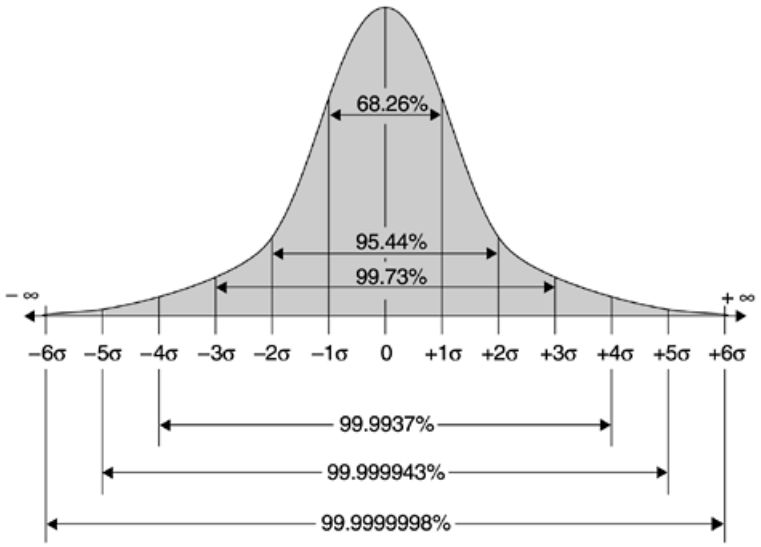

Figure 4.17: Gaussian distribution with some specific standard deviation values. These deviations represent the possibility of a new physics hypothesis is true against the background only hypothesis. The figure is taken from [61].

The most simple and common relation for significance calculations is

$$Z = s/\sqrt{b} \tag{4.2}$$

where Z is the expected discovery significance, s is stands for signal and b is background. What about if we have uncertainty for background? For such a case, only the uncertainty of background is relevant for calculation, though signal uncertainty is used only for setting limits [62]. In this perspective, equation 4.2 is modified as

$$Z = s/\sqrt{b + \sigma_b^2} \tag{4.3}$$

where σ_b^2 is the variance of background and represented as

$$\sigma_b = (uncertainty) \times b \tag{4.4}$$

For instance, if backgrounds have a 25% uncertainty, explicit version of equation 4.3

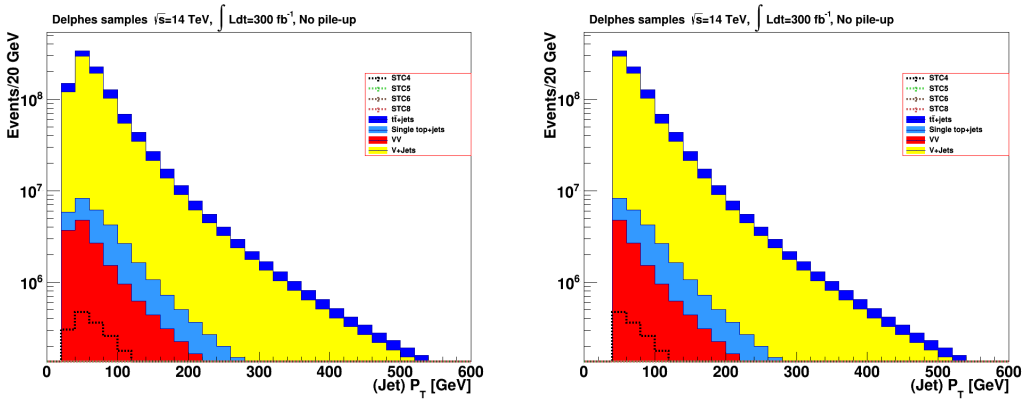

(a) Jet p_T distributions before cut

(b) Jet p_T distributions after cut

Figure 4.18: Jet p_T distributions before and after $p_T > 40$ GeV cut for No pile-up case

becomes

$$Z = s/\sqrt{b + (0.25 \times b)^2} \tag{4.5}$$

[63].

4.7 Control plots and Inclusive Variables

Requiring at least 4 (6) jets for direct top squark pair production (gluino associated stop pair production) with $p_T > 40$ GeV and $|\eta|$ <2.4 increases the fraction of $\tilde{t}_1\tilde{t}_1^*$ events with respect to $\tilde{b}_1\tilde{b}_1^*$ events, which are the main SUSY background as stated in previous section [60]. Also, the events with lepton transverse momentum is bigger than 20 GeV are selected. These cuts are the classical cuts that are used similarly almost all the single lepton searches. In the figures 4.18, 4.19, and 4.20, jet transverse momentum distributions with the corresponding cut are shown. In the figures 4.21, 4.22, and 4.23, lepton transverse momentum distributions with the corresponding cut are shown, respectively.

Just after the multiplicity, transverse momentum and pseudorapidity cuts, $E_T^{miss} > 500$ GeV is applied, because there is additional missing energy due to the additional

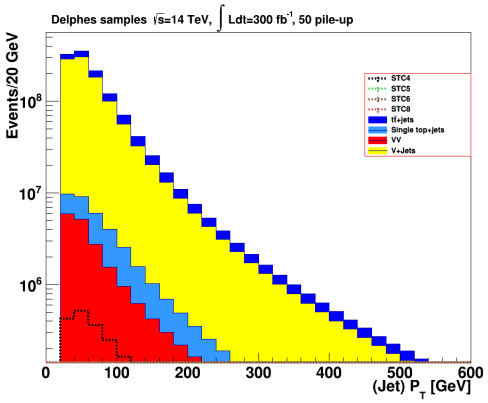

(a) Jet p_T distributions before cut

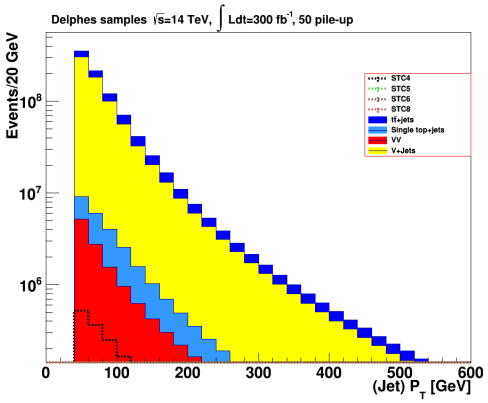

(b) Jet p_T distributions after cut

Figure 4.19: Jet p_T distributions before and after $p_T > 40$ GeV cut for 50 pile-up case

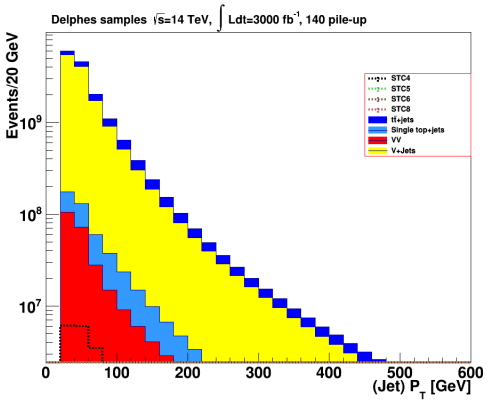

(a) Jet p_T distributions before cut

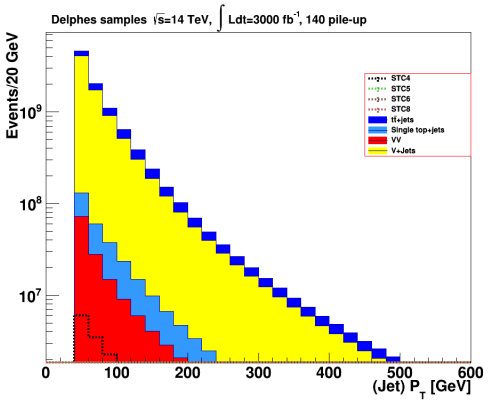

(b) Jet p_T distributions after cut

Figure 4.20: Jet p_T distributions before and after $p_T > 40$ GeV cut for 140 pile-up case

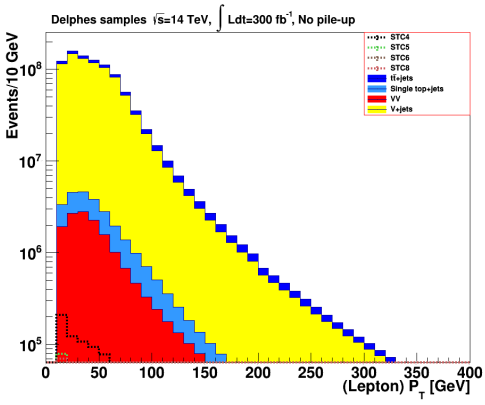

(a) Lepton p_T distributions before cut

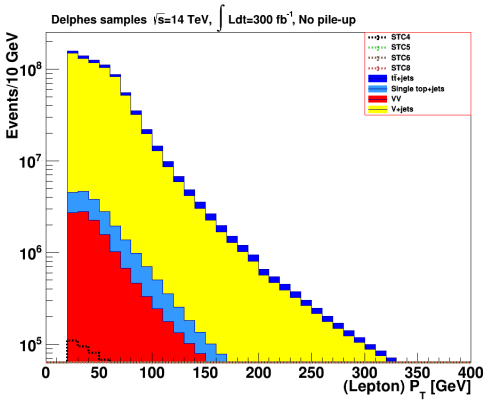

(b) Lepton p_T distributions after cut

Figure 4.21: Lepton p_T distributions before and after $p_T > 20$ GeV cut for No pile-up case

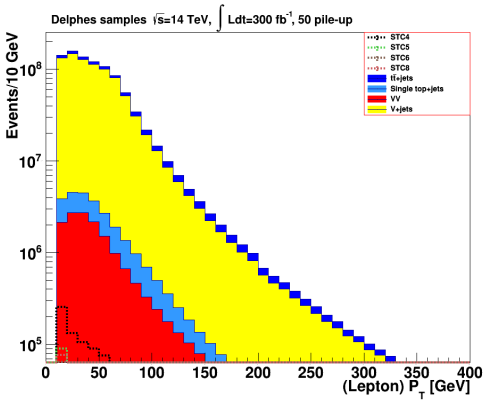

(a) Lepton p_T distributions before cut

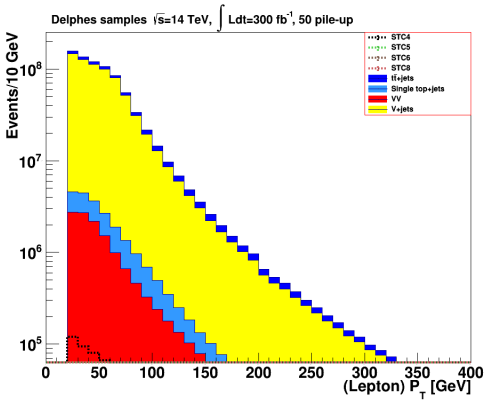

(b) Lepton p_T distributions after cut

Figure 4.22: Lepton p_T distributions before and after $p_T > 20$ GeV cut for 50 pile-up case

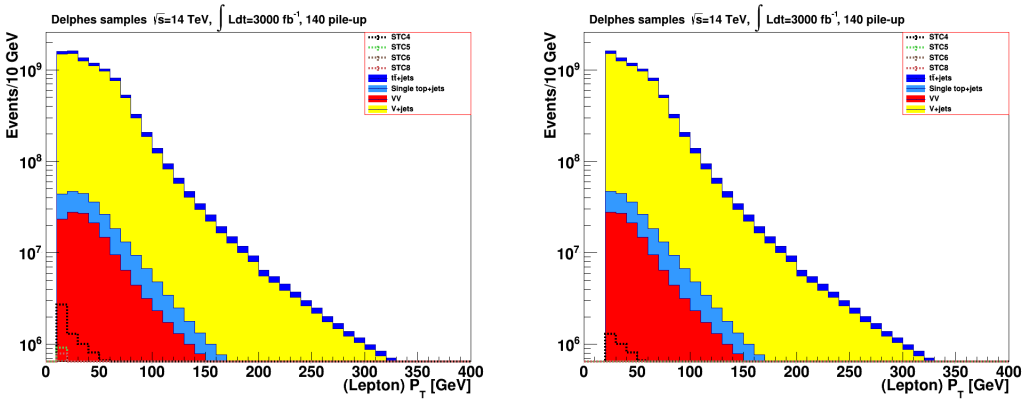

(a) Lepton p_T distributions before cut

(b) Lepton p_T distributions after cut

Figure 4.23: Lepton p_T distributions before and after $p_T > 20$ GeV cut for 140 pile-up case

neutralinos and neutrinos. E_T^{miss} is an inclusive variable and one of the common variables used for SUSY searches since it is expected to find signal events in higher missing energy region. In the figures 4.24, 4.25, and 4.26, E_T^{miss} distributions before and after the $E_T^{miss} > 500$ GeV cut are shown for each pile-up cases, respectively.

To reduce SM background further, a new angular variable, min $\Delta\phi$ which is introduced in [60], is used. min $\Delta\phi$ is the minimum angle between the leading jet and E_T^{miss} in the azimuthal plane. $\Delta\phi$ value is small for QCD multi jet background whereas signal points are expected have larger values, and this makes the variable useful for our analysis. In the tables 4.1, 4.2, and 4.3, the significance results after the $\Delta\phi$ cut are shown for each signal scenarios and for each pile-up cases. The significance results are below 2σ which is too low to be considered enough for a discovery.

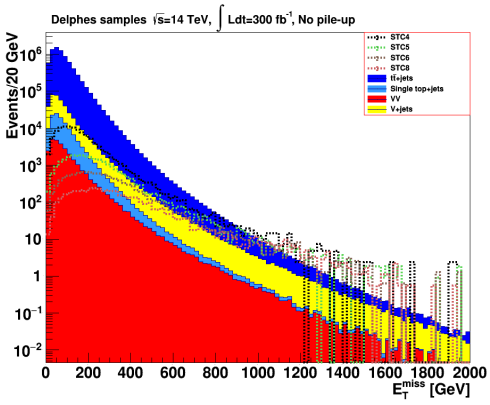

(a) E_T^{miss} distributions before cut

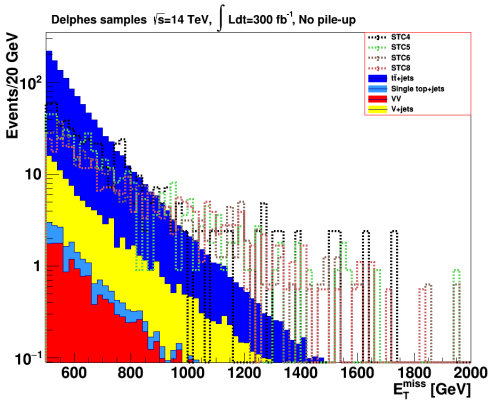

(b) E_T^{miss} distributions after cut

Figure 4.24: E_T^{miss} distributions before and after $E_T^{miss} > 500$ GeV cut for No pile-up case

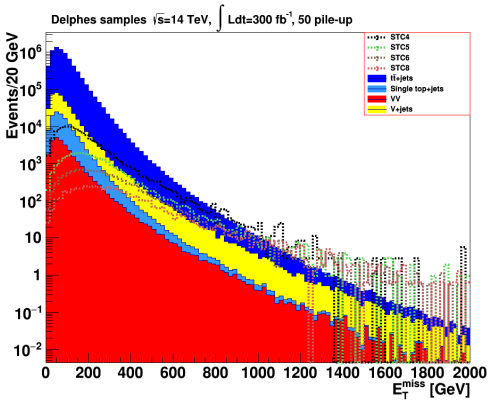

(a) E_T^{miss} distributions before cut

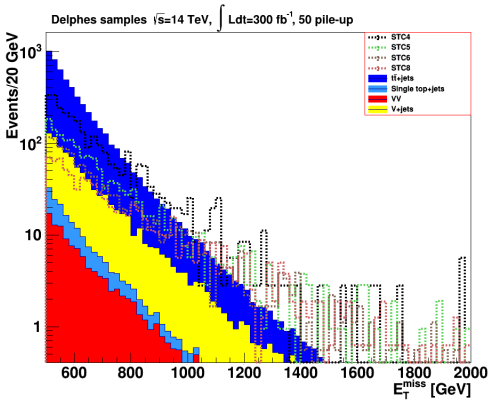

(b) E_T^{miss} distributions after cut

Figure 4.25: E_T^{miss} distributions before and after $E_T^{miss} > 500$ GeV cut for 50 pile-up case

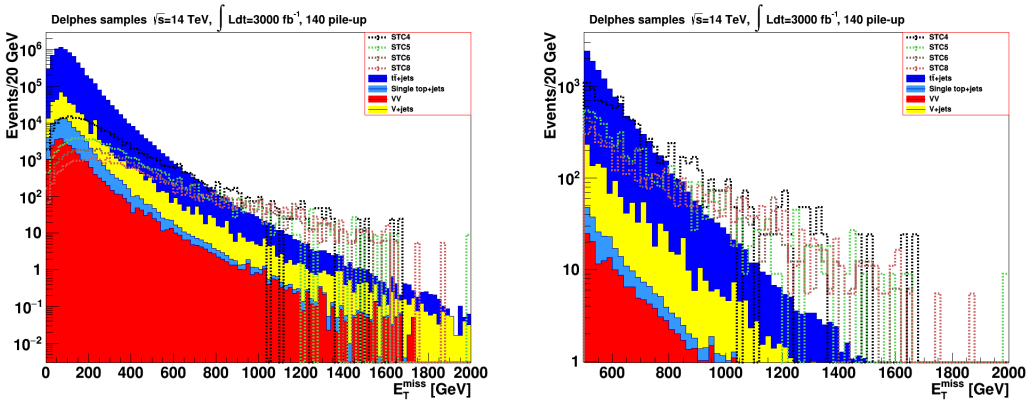

(a) E_T^{miss} distributions before cut

(b) E_T^{miss} distributions after cut

Figure 4.26: E_T^{miss} distributions before and after $E_T^{miss} > 500$ GeV cut for 140 pile-up case

No pile-up events, $300fb^{-1}$									
Selection	diboson	boson+jets	$t\bar{t}$+jets	single top	sum bgrds	STC4	STC5	STC6	STC8
preselection	1x10^8	2x10^{10}	2x10^8	6x10^7	2x10^{10}	4x10^6	1x10^6	759000	873000
single lepton	1x10^7	7x10^8	5x10^7	1x10^7	8x10^8	588811	166533	99670	100445
# of Jets>=4	289598	5x10^6	1x10^7	184833	2x10^7	208990	46927	19368	9217
# of b-Jets>=2	26482	263585	7x10^6	96335	7x10^6	107590	25816	10971	4622
E_T^{miss}>500	108	681	4146	69	5004	2050	1341	1003	751
$\Delta\phi > 0.5$	101	640	3454	56	4251	1493	1107	856	665
$s/\sqrt{b+(0.25\times b)^2}$						1.4	1.0	0.8	0.6
$s/\sqrt{b+(0.15\times b)^2}$						2.3	1.7	1.3	1.0

Table 4.1: Significance of signal just after the $\Delta\phi$ cut for no pile-up scenario.

50 pile-up events, $300fb^{-1}$									
Selection	diboson	boson+jets	$t\bar{t}$+jets	single top	sum bgrds	STC4	STC5	STC6	STC8
preselection	1x10^8	2x10^{10}	2x10^8	6x10^7	2x10^{10}	4x10^6	1x10^6	759000	873000
single lepton	1x10^7	7x10^8	5x10^7	9x10^6	8x10^8	592036	164640	97957	98218
# of Jets>=4	317609	6x10^6	1x10^7	210947	2x10^7	199416	48327	20562	9798
# of b-Jets>=2	27423	288751	7x10^6	101471	7x10^6	100444	26398	11610	4931
E_T^{miss}>500	110	701	4373	77	5261	2710	1453	1073	807
$\Delta\phi > 0.5$	102	654	3646	63	4465	1909	1185	912	714
$s/\sqrt{b+(0.25\times b)^2}$						1.7	1.1	0.8	0.6
$s/\sqrt{b+(0.15\times b)^2}$						2.8	1.8	1.4	1.1

Table 4.2: Significance of signal just after the $\Delta\phi$ cut for 50 pile-up scenario.

140 pile-up events, $3000 fb^{-1}$									
Selection	diboson	boson+jets	$t\bar{t}$+jets	single top	sum bgrds	STC4	STC5	STC6	STC8
preselection	1x10^9	2x10^{11}	2x10^9	6x10^8	2x10^{11}	4x10^7	1x10^7	8x10^6	9x10^6
single lepton	1x10^8	7x10^9	5x10^8	1x10^8	8x10^9	6x10^6	2x10^6	983358	980090
# of Jets>=6	208573	4x10^6	1x10^7	138356	1x10^7	316176	95593	51790	30386
# of b-Jets>=2	24376	275394	7x10^6	67610	7x10^6	183552	59288	34094	21181
E_T^{miss}>500	159	1034	11166	115	12474	9624	5014	4272	3803
$\Delta\phi > 0.5$	148	963	9434	95	10640	7296	4235	3538	3388
$s/\sqrt{b + (0.25 \times b)^2}$						2.7	1.6	1.3	1.3
$s/\sqrt{b + (0.15 \times b)^2}$						4.6	2.6	2.2	2.1

Table 4.3: Significance of signal just after the $\Delta\phi$ cut for 140 pile-up scenario.

No pile-up events, $300 fb^{-1}$									
Selection	diboson	boson+jets	$t\bar{t}$+jets	single top	sum bgrds	STC4	STC5	STC6	STC8
preselection	1x10^8	2x10^{10}	2x10^8	6x10^7	2x10^{10}	4x10^6	1x10^6	759000	873000
single lepton	1x10^7	7x10^8	5x10^7	1x10^7	8x10^8	588811	166533	99670	100445
# of Jets>=4	289598	5x10^6	1x10^7	184833	2x10^7	208990	46927	19368	9217
# of b-Jets>=2	26482	263585	7x10^6	96335	7x10^6	107590	25816	10971	4622
E_T^{miss}>500	108	681	4146	69	5004	2050	1341	1003	751
$\Delta\phi > 0.5$	101	640	3454	56	4251	1493	1107	856	665
$H_T > 1100$	43	272	1438	26	1779	1070	656	488	434
$s/\sqrt{b + (0.25 \times b)^2}$						2.4	1.5	1.1	1.0
$s/\sqrt{b + (0.15 \times b)^2}$						4.0	2.4	1.8	1.6

Table 4.4: Significance of signal just after the H_T cut for no pile-up scenario.

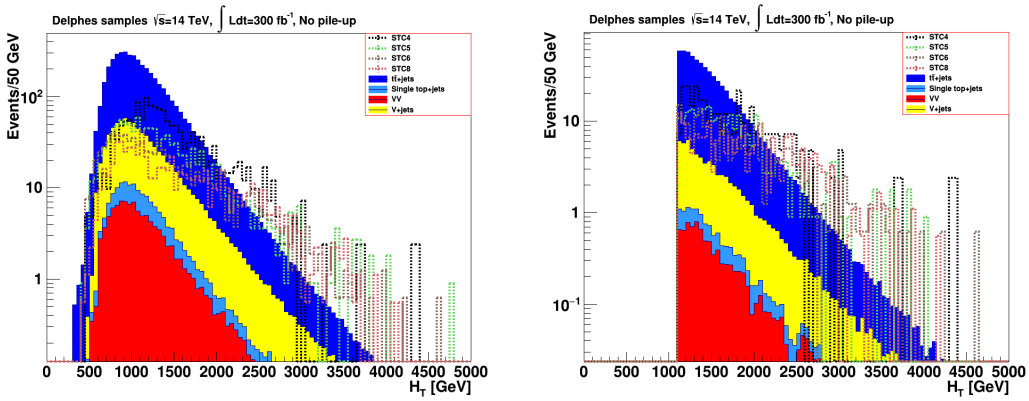

(a) H_T distributions before cut

(b) H_T distributions after cut

Figure 4.27: H_T distributions before and after $H_T > 1100$ GeV cut for No pile-up case

To eliminate the background and increase the significance of the signal more, another common SUSY search variable, H_T is used. It is an inclusive variable just like E_T^{miss} and described as the scalar sum of the jet transverse momentum values. As it can be seen in Figure 4.27, Figure 4.28, and Figure 4.29, a hard cut on H_T can effectively separate the signal from the background. It can be seen in the tables 4.4, 4.5, and 4.6 that just after the H_T cut, the biggest remaining background is dileptonic $t\bar{t}$ decays with one of the leptons is missing.

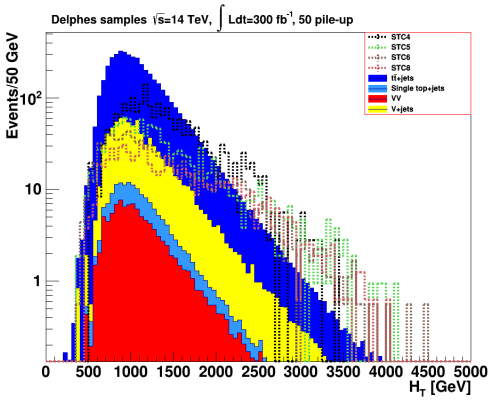

(a) H_T distributions before cut

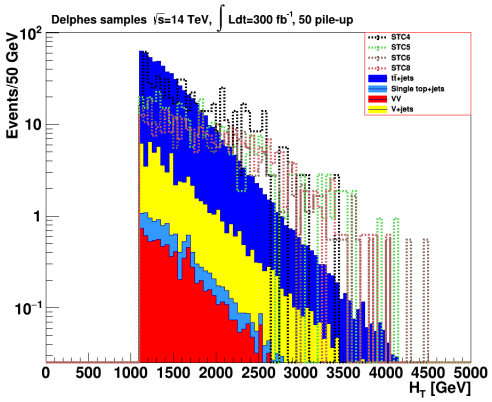

(b) H_T distributions after cut

Figure 4.28: H_T distributions before and after $H_T > 1100$ GeV cut for 50 pile-up case

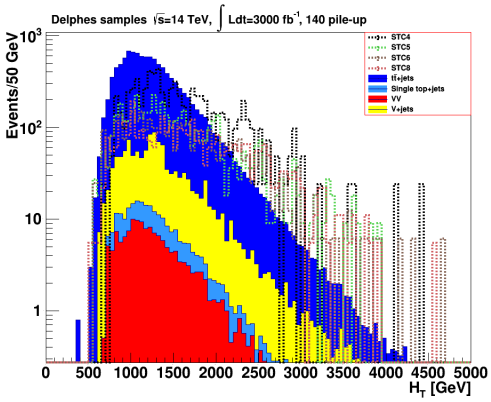

(a) H_T distributions before cut

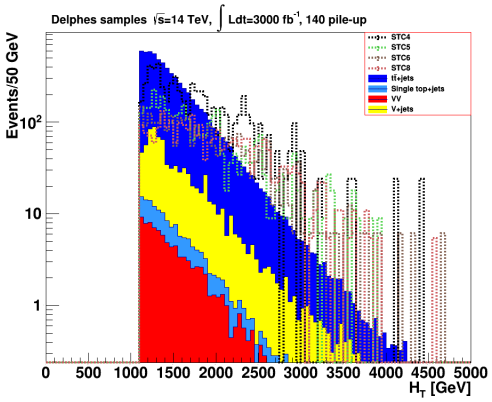

(b) H_T distributions after cut

Figure 4.29: H_T distributions before and after $H_T > 1100$ GeV cut for 140 pile-up case

50 pile-up events, $300 fb^{-1}$									
Selection	diboson	boson+jets	$t\bar{t}$+jets	single top	sum bgrds	STC4	STC5	STC6	STC8
preselection	1x10^8	2x10^{10}	2x10^8	6x10^7	2x10^{10}	4x10^6	1x10^6	759000	873000
single lepton	1x10^7	7x10^8	5x10^7	9x10^6	8x10^8	592036	164640	97957	98218
# of Jets>=4	317609	6x10^6	1x10^7	210947	2x10^7	199416	48327	20562	9798
# of b-Jets>=2	27423	288751	7x10^6	101471	7x10^6	100444	26398	11610	4931
E_T^{miss}>500	110	701	4373	77	5261	2710	1453	1073	807
$\Delta\phi > 0.5$	102	654	3646	63	4465	1909	1185	912	714
$H_T > 1100$	42	269	1480	27	1818	1294	704	508	463
$s/\sqrt{b + (0.25 \times b)^2}$						2.8	1.5	1.1	1.0
$s/\sqrt{b + (0.15 \times b)^2}$						4.7	2.6	1.8	1.7

Table 4.5: Significance of signal just after the H_T cut for 50 pile-up scenario.

140 pile-up events, $3000 fb^{-1}$									
Selection	diboson	boson+jets	$t\bar{t}$+jets	single top	sum bgrds	STC4	STC5	STC6	STC8
preselection	1x10^9	2x10^{11}	2x10^9	6x10^8	2x10^{11}	4x10^7	1x10^7	8x10^6	9x10^6
single lepton	1x10^8	7x10^9	5x10^8	1x10^8	8x10^9	6x10^6	2x10^6	983358	980090
# of Jets>=6	208573	4x10^6	1x10^7	138356	1x10^7	316176	95593	51790	30386
# of b-Jets>=2	24376	275394	7x10^6	67610	7x10^6	183552	59288	34094	21181
E_T^{miss}>500	159	1034	11166	115	12474	9624	5014	4272	3803
$\Delta\phi > 0.5$	148	963	9434	95	10640	7296	4235	3538	3388
$H_T > 1100$	91	647	5604	61	6403	5928	3089	2589	2586
$s/\sqrt{b + (0.25 \times b)^2}$						3.7	1.9	1.6	1.6
$s/\sqrt{b + (0.15 \times b)^2}$						6.2	3.2	2.7	2.7

Table 4.6: Significance of signal just after the H_T cut for 140 pile-up scenario.

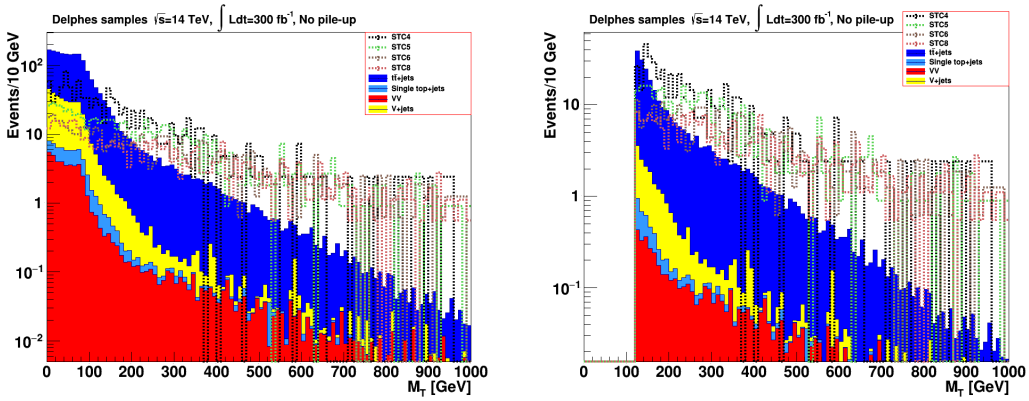

(a) M_T distributions before cut

(b) M_T distributions after cut

Figure 4.30: M_T distributions before and after $M_T > 120$ GeV cut for No pile-up case

Boson+jet background, which is a lepton, E_T^{miss} and jet source was the biggest background before the previous cuts. Yet now, it is very small compared to $t\bar{t}$, but still not negligible. Here E_T^{miss} is originated from the single neutrino of leptonic boson, mostly W, decay. Since it is single boson decay, a cut on M_T distribution can eliminate such backgrounds due to the fact that M_T distribution has an end point at the W boson mass. In the figures 4.30, 4.31, and 4.32, M_T distributions are shown. In Table 4.7, Table 4.8, and Table 4.9, the signal significance values obtained after the M_T cut are shown, respectively.

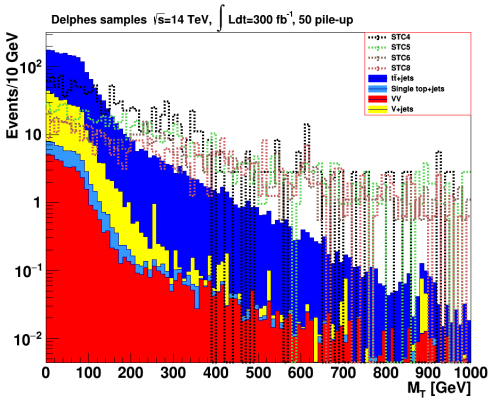

(a) M_T distributions before cut

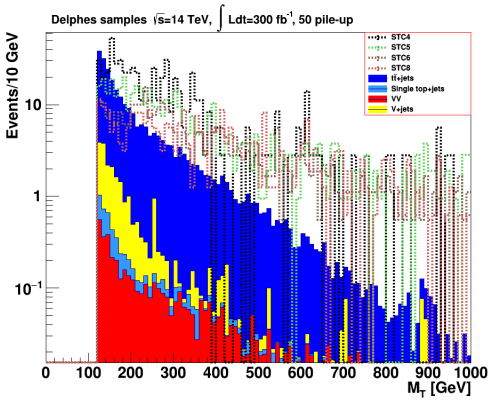

(b) M_T distributions after cut

Figure 4.31: M_T distributions before and after $M_T > 120$ GeV cut for 50 pile-up case

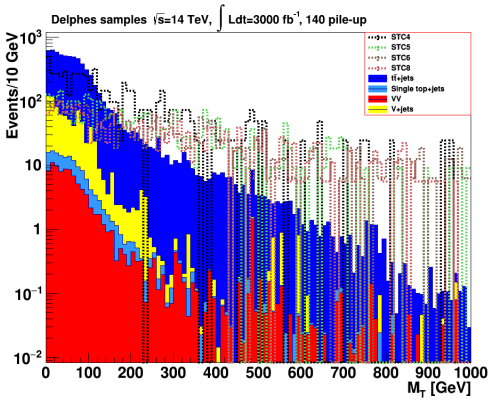

(a) M_T distributions before cut

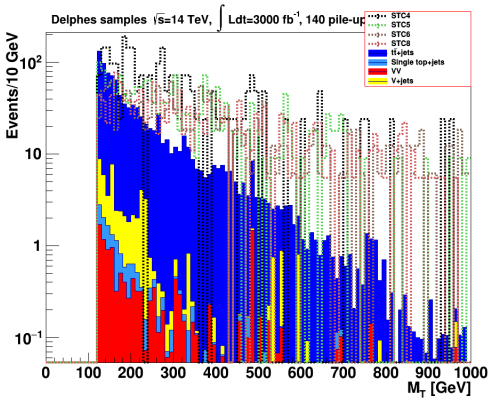

(b) M_T distributions after cut

Figure 4.32: M_T distributions before and after $M_T > 120$ GeV cut for 140 pile-up case

No pile-up events, $300 fb^{-1}$									
Selection	diboson	boson+jets	$t\bar{t}$+jets	single top	sum bgrds	STC4	STC5	STC6	STC8
preselection	1x10^8	2x10^{10}	2x10^8	6x10^7	2x10^{10}	4x10^6	1x10^6	759000	873000
single lepton	1x10^7	7x10^8	5x10^7	1x10^7	8x10^8	588811	166533	99670	100445
# of Jets>=4	289598	5x10^6	1x10^7	184833	2x10^7	208990	46927	19368	9217
# of b-Jets>=2	26482	263585	7x10^6	96335	7x10^6	107590	25816	10971	4622
E_T^{miss}>500	108	681	4146	69	5004	2050	1341	1003	751
$\Delta\phi > 0.5$	101	640	3454	56	4251	1493	1107	856	665
$H_T > 1100$	43	272	1438	26	1779	1070	656	488	434
$M_T > 120$	5	14	229	2	250	554	406	330	291
$s/\sqrt{b + (0.25 \times b)^2}$						8.6	6.3	5.1	4.5
$s/\sqrt{b + (0.15 \times b)^2}$						13.6	10.0	8.1	2.7

Table 4.7: Number of events remaining just after the M_T cut for no pile-up scenario and the significance results.

50 pile-up events, $300 fb^{-1}$									
Selection	diboson	boson+jets	$t\bar{t}$+jets	single top	sum bgrds	STC4	STC5	STC6	STC8
preselection	1x10^8	2x10^{10}	2x10^8	6x10^7	2x10^{10}	4x10^6	1x10^6	759000	873000
single lepton	1x10^7	7x10^8	5x10^7	9x10^6	8x10^8	592036	164640	97957	98218
# of Jets>=4	317609	6x10^6	1x10^7	210947	2x10^7	199416	48327	20562	9798
# of b-Jets>=2	27423	288751	7x10^6	101471	7x10^6	100444	26398	11610	4931
E_T^{miss}>500	110	701	4373	77	5261	2710	1453	1073	807
$\Delta\phi > 0.5$	102	654	3646	63	4465	1909	1185	912	714
$H_T > 1100$	42	269	1480	27	1818	1294	704	508	463
$M_T > 120$	5	16	230	2	253	665	449	343	317
$s/\sqrt{b + (0.25 \times b)^2}$						10.2	6.9	5.3	4.9
$s/\sqrt{b + (0.15 \times b)^2}$						16.2	10.9	8.3	7.7

Table 4.8: Number of events remaining just after the M_T cut for 50 pile-up scenario and the significance results.

140 pile-up events, $3000 fb^{-1}$									
Selection	diboson	boson+jets	$t\bar{t}$+jets	single top	sum bgrds	STC4	STC5	STC6	STC8
preselection	1x10^9	2x10^{11}	2x10^9	6x10^8	2x10^{11}	4x10^7	1x10^7	8x10^6	9x10^6
single lepton	1x10^8	7x10^9	5x10^8	1x10^8	8x10^9	6x10^6	2x10^6	983358	980090
# of Jets>=6	208573	4x10^6	1x10^7	138356	1x10^7	316176	95593	51790	30386
# of b-Jets>=2	24376	275394	7x10^6	67610	7x10^6	183552	59288	34094	21181
E_T^{miss}>500	159	1034	11166	115	12474	9624	5014	4272	3803
$\Delta\phi > 0.5$	148	963	9434	95	10640	7296	4235	3538	3388
$H_T > 1100$	91	647	5604	61	6403	5928	3089	2589	2586
$M_T > 120$	14	39	908	6	967	2784	1952	1720	1773
$s/\sqrt{b + (0.25 \times b)^2}$						11.4	8.0	7.1	7.3
$s/\sqrt{b + (0.15 \times b)^2}$						18.8	13.2	11.6	12.0

Table 4.9: Number of events remaining just after the M_T cut for 140 pile-up scenario and the significance results.

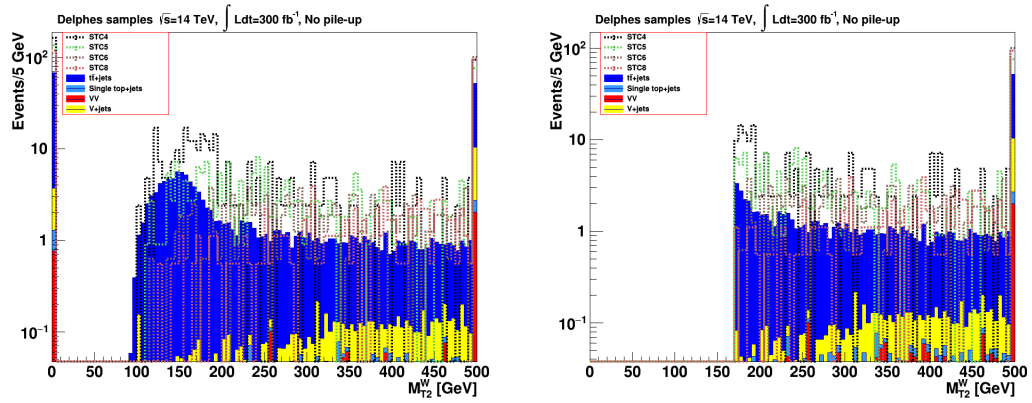

(a) M_{T2}^{W} distributions before cut

(b) M_{T2}^{W} distributions after cut

Figure 4.33: M_{T2}^{W} distributions before and after $M_{T2}^{W} > 170$ GeV cut for No pile-up case

4.8 Analysis with the Dedicated Variables, and Their Comparison

After the cuts mentioned previous section, the largest remaining background is dileptonic $t\bar{t}$ channel. The results are in good agreement with the results of ATLAS $t\bar{t}$ research [64] up to now.

However, since E_T^{miss} and H_T cuts are composite variables, it can be deduced that the previous cuts may not sort out the signal efficiently and correctly enough. In addition, the last cut, M_T, is for one W boson decay branch with one missing particle. Yet, there are more than one W boson decay branches with more than one missing particle. So, at this point, we need exclusive variables to go further in our analysis. These variables are M_{T2}^{W} and topness (t) whose mathematical descriptions and physical meanings are described in Chapter 3. In the figures 4.33, 4.34, and 4.35, event distribution for M_{T2}^{W}, before and after cuts, are shown. In the figures 4.36, 4.37, and 4.38, event distribution for topness, before and after cuts, are shown.

In the tables 4.10, 4.11, and 4.12, for each pile-up scenario and each STC models, significance results of M_{T2}^{W} and topness variables can be seen separately. In the cut flow, M_{T2}^{W} and topness are applied after the previous cuts and these two are applied interchangeably.

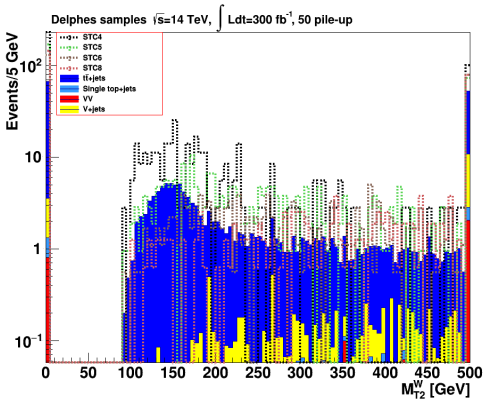

(a) M_{T2}^{W} distributions before cut

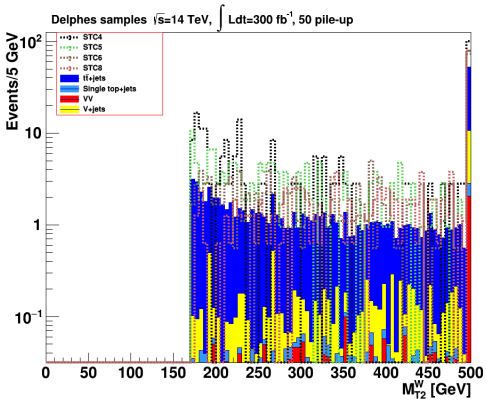

(b) M_{T2}^{W} distributions after cut

Figure 4.34: M_{T2}^{W} distributions before and after $M_{T2}^{W} > 170$ GeV cut for 50 pile-up case

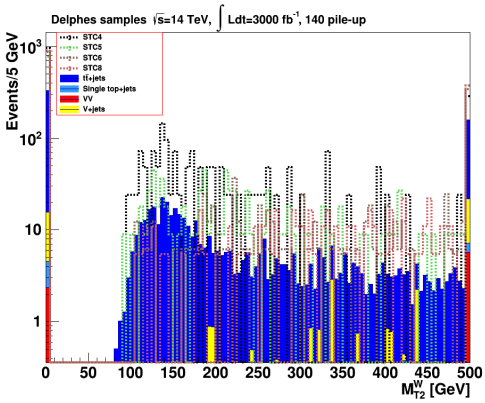

(a) M_{T2}^{W} distributions before cut

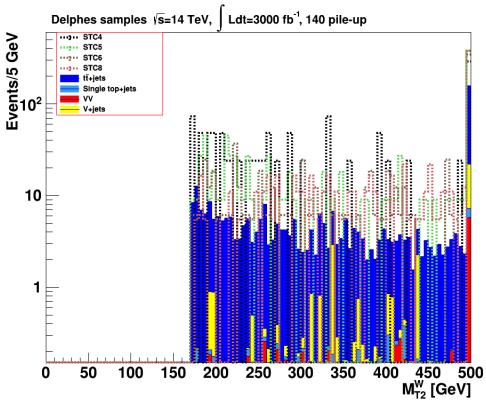

(b) M_{T2}^{W} distributions after cut

Figure 4.35: M_{T2}^{W} distributions before and after $M_{T2}^{W} > 170$ GeV cut for 140 pile-up case

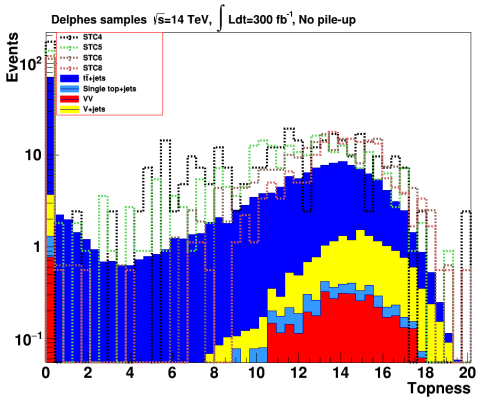

(a) Topness distributions before cut

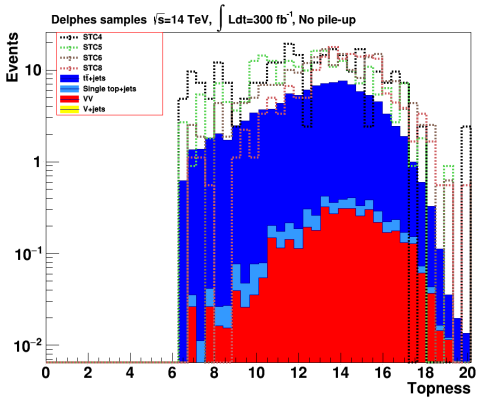

(b) Topness distributions after cut

Figure 4.36: Topness distributions before and after $t > 6.5$ cut for No pile-up case

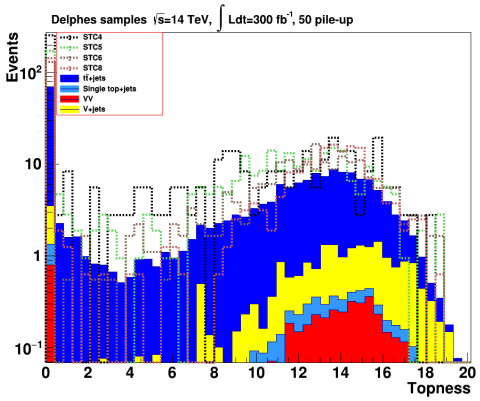

(a) Topness distributions before cut

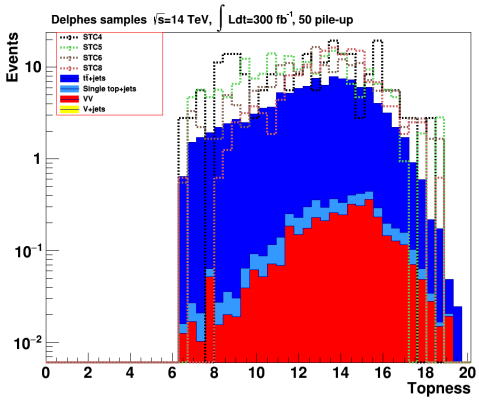

(b) Topness distributions after cut

Figure 4.37: Topness distributions before and after $t > 6.5$ cut for 50 pile-up case

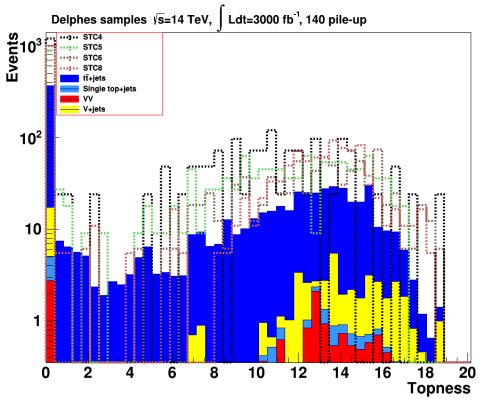

(a) Topness distributions before cut

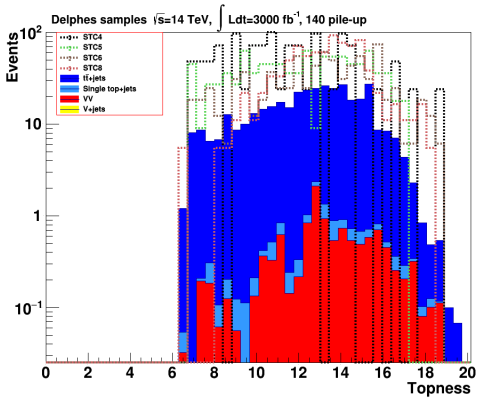

(b) Topness distributions after cut

Figure 4.38: Topness distributions before and after $t > 6.5$ cut for 140 pile-up case

No pile-up events, $300fb^{-1}$									
Selection	diboson	boson+jets	$t\bar{t}$+jets	single top	sum bgrds	STC4	STC5	STC6	STC8
preselection	1x10^8	2x10^{10}	2x10^8	6x10^7	2x10^{10}	4x10^6	1x10^6	759000	873000
single lepton	1x10^7	7x10^8	5x10^7	1x10^7	8x10^8	588811	166533	99670	100445
# of Jets>=4	289598	5x10^6	1x10^7	184833	2x10^7	208990	46927	19368	9217
# of b-Jets>=2	26482	263585	7x10^6	96335	7x10^6	107590	25816	10971	4622
MET>500	108	681	4146	69	5004	2050	1341	1003	751
$\Delta\phi > 0.5$	101	640	3454	56	4251	1493	1107	856	665
$H_T > 1100$	43	272	1438	26	1779	1070	656	488	434
$M_T > 120$	5	14	229	2	250	554	406	330	291
$M_{T2}^W > 170$	4	12	111	1	128	286	238	210	170
$s/\sqrt{b+(0.25\times b)^2}$ for M_{T2}^W						8.4	7.0	6.2	5.0
$s/\sqrt{b+(0.15\times b)^2}$ for M_{T2}^W						12.8	10.7	9.4	7.6
$topness > 6.5$	4	12	102	1	119	252	218	208	169
$s/\sqrt{b+(0.25\times b)^2}$ for topness						8.0	6.9	6.6	5.3
$s/\sqrt{b+(0.15\times b)^2}$ for topness						12.1	10.4	9.9	8.1

Table 4.10: Significance of signal after the M_{T2}^W and topness cuts interchangeably for no pile-up scenario. There are two options for background uncertainty, and results are evaluated for both of them separately.

50 pile-up events, $300 fb^{-1}$									
Selection	diboson	boson+jets	$t\bar{t}$+jets	single top	sum bgrds	STC4	STC5	STC6	STC8
preselection	1x10^8	2x10^{10}	2x10^8	6x10^7	2x10^{10}	4x10^6	1x10^6	759000	873000
single lepton	1x10^7	7x10^8	5x10^7	9x10^6	8x10^8	592036	164640	97957	98218
# of Jets>=4	317609	6x10^6	1x10^7	210947	2x10^7	199416	48327	20562	9798
# of b-Jets>=2	27423	288751	7x10^6	101471	7x10^6	100444	26398	11610	4931
MET>500	110	701	4373	77	5261	2710	1453	1073	807
$\Delta\phi > 0.5$	102	654	3646	63	4465	1909	1185	912	714
$H_T > 1100$	42	269	1480	27	1818	1294	704	508	463
$M_T > 120$	5	16	230	2	253	665	449	343	317
$M_{T2}^W > 170$	4	14	114	2	134	264	228	191	164
$s/\sqrt{b + (0.25 \times b)^2}$ for M_{T2}^W						7.4	6.4	5.4	4.6
$s/\sqrt{b + (0.15 \times b)^2}$ for M_{T2}^W						11.4	9.8	8.2	7.1
$topness > 6.5$	4	14	105	1	124	225	210	182	161
$s/\sqrt{b + (0.25 \times b)^2}$ for topness						6,8	6.4	5.5	4.9
$s/\sqrt{b + (0.15 \times b)^2}$ for topness						10.4	9.7	8.4	7.4

Table 4.11: Significance of signal after the M_{T2}^W and topness cuts interchangeably for 50 pile-up scenario. There are two options for background uncertainty, and results are evaluated for both of them separately.

140 pile-up events, $3000 fb^{-1}$									
Selection	diboson	boson+jets	$t\bar{t}$+jets	single top	sum bgrds	STC4	STC5	STC6	STC8
preselection	1x10^9	2x10^{11}	2x10^9	6x10^8	2x10^{11}	4x10^7	1x10^7	8x10^6	9x10^6
single lepton	1x10^8	7x10^9	5x10^8	1x10^8	8x10^9	6x10^6	2x10^6	983358	980090
# of Jets>=6	208573	4x10^6	1x10^7	138356	1x10^7	316176	95593	51790	30386
# of b-Jets>=2	24376	275394	7x10^6	67610	7x10^6	183552	59288	34094	21181
MET>500	159	1034	11166	115	12474	9624	5014	4272	3803
$\Delta\phi > 0.5$	148	963	9434	95	10640	7296	4235	3538	3388
$H_T > 1100$	91	647	5604	61	6403	5928	3089	2589	2586
$M_T > 120$	14	39	908	6	967	2784	1952	1720	1773
$M_{T2}^W > 170$	11	27	386	4	428	1104	958	796	829
$s/\sqrt{b + (0.25 \times b)^2}$ for M_{T2}^W						10.1	8.8	7.3	7.6
$s/\sqrt{b + (0.15 \times b)^2}$ for M_{T2}^W						16.4	14.2	11.8	12.3
$topness > 6.5$	11	27	356	3	397	1032	895	771	813
$s/\sqrt{b + (0.25 \times b)^2}$ for topness						10.2	8.4	7.6	8.0
$s/\sqrt{b + (0.15 \times b)^2}$ for topness						16.4	14.3	12.3	13.0

Table 4.12: Significance of signal after the M_{T2}^W and topness cuts interchangeably for 140 pile-up scenario. There are two options for background uncertainty, and results are evaluated for both of them separately.

The results are promising. $t\bar{t}$ background decreases to its half, and the significance results of all the signal scenarios are above the 5σ for all the possible cases. When using the improved uncertainty, 15%, significance results almost increase by its one and a half as expected, because improved uncertainty means we are much closer to the realistic result in the hypothesis that SUSY exits. In addition, the results of these two variables are almost the same. That means, both of them can be used separately or together in the analyses. In the figures 4.39, 4.40, and 4.41, trend of the increased significance results are shown for 15% background uncertainty, respectively. Numbers on the horizontal axises represents the important cuts; $\Delta\phi$, H_T, M_T, and M_{T2}^W or topness respectively. Each significance value represents the significance of the signal just after the corresponding cut. After the 3^{rd} cut, M_T, significance reaches its maximum value for all the cases, and then decreases after the dedicated variables. However, it doesn't mean that stransverse mass and topness is not working properly. The reason for the decrease might be that M_T cut separates background and signal wrongly. M_T is used for calculating the mother particle mass with the information of daughter particles. For instance, W boson mass is obtained with the lepton and the missing neutrino by using the transverse variables. As it is explained in Chapter 3, since there are more than one missing particles, the system is underconstrained for M_T. As a result, M_T might not tag the signal and background efficiently enough so that it gives us fake results.

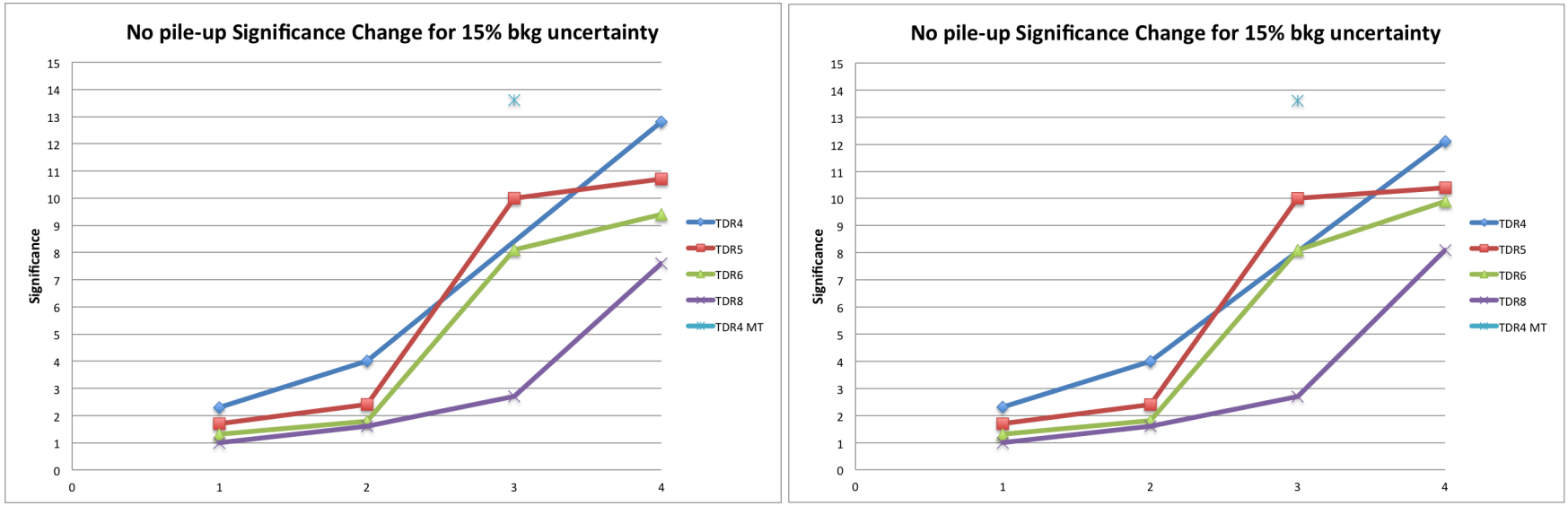

(a) Cutflow that includes M_{T2}^{W}

(b) Cutflow that includes topness

Figure 4.39: Significance vs. corresponding cuts plot for the collision with no pile-up. It shows us the improvement in the significance after each cut. On the horizontal axis, 1 stands for $\Delta\phi$, 2 is for H_T, 3 is for M_T, and 4 is for M_{T2}^{W} (a) or topness (b). Dots are linked to one another via straight lines to show us the increase in the significance more clearly. 3^{rd} cut, M_T, is excluded, because it is highly possible that M_T tags signal and background events wrongly.

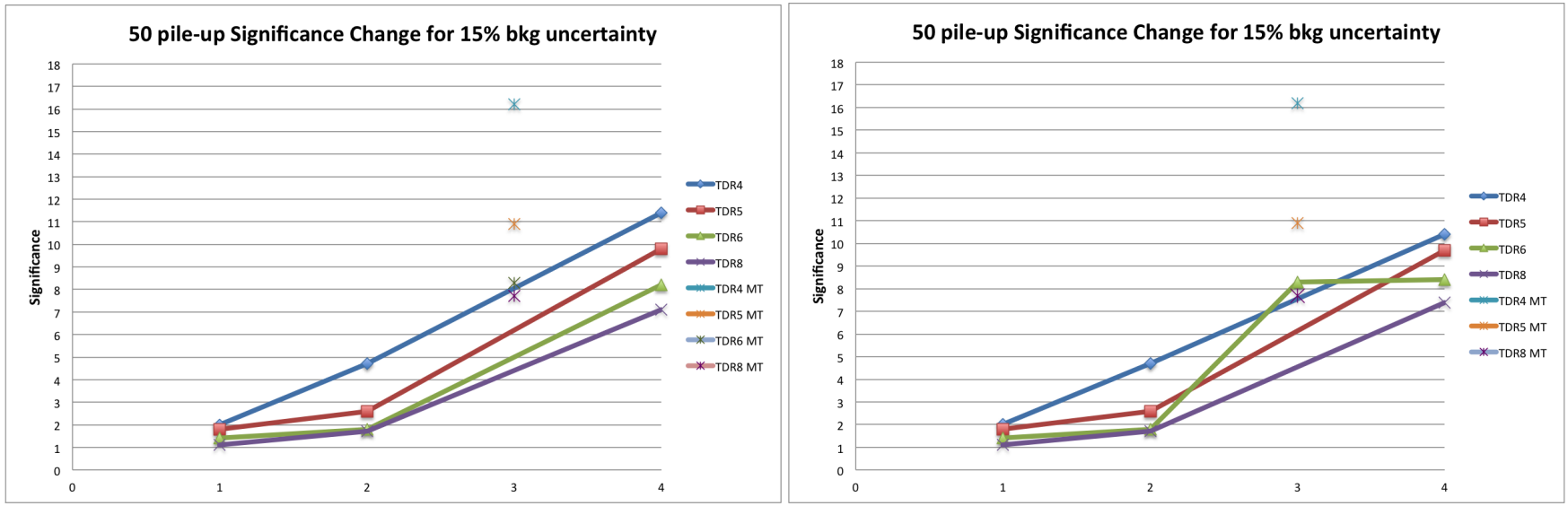

(a) Cutflow that includes M_{T2}^{W}

(b) Cutflow that includes topness

Figure 4.40: Significance vs. corresponding cuts plot for the collision with no pile-up. It shows us the improvement in the significance after each cut. On the horizontal axis,1 stands for $\Delta\phi$, 2 is for H_T, 3 is for M_T, and 4 is for M_{T2}^{W} (a) or topness (b). Dots are linked to one another via straight lines to show us the increase in the significance more clearly. 3^{rd} cut, M_T, is excluded, because it is highly possible that M_T tags signal and background events wrongly.

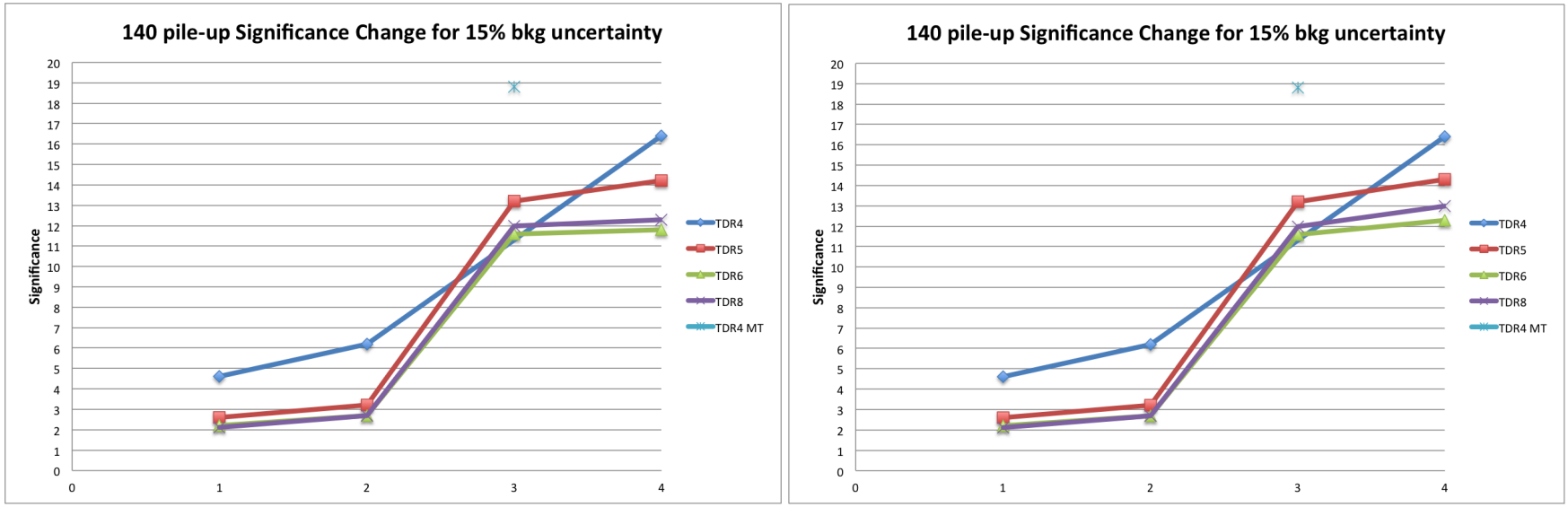

(a) Cutflow that includes M_{T2}^{W}

(b) Cutflow that includes topness

Figure 4.41: Significance vs. corresponding cuts plot for the collision with no pile-up. It shows us the improvement in the significance after each cut. On the horizontal axis,1 stands for $\Delta\phi$, 2 is for H_T, 3 is for M_T, and 4 is for M_{T2}^{W} (a) or topness (b). Dots are linked to one another via straight lines to show us the increase in the significance more clearly. 3^{rd} cut, M_T, is excluded, because it is highly possible that M_T tags signal and background events wrongly.

CHAPTER 5

CONCLUSION

In conclusion, this thesis contributes to the searches for the answers to the most important questions in particle physics; what are the exact symmetry and the laws of the Universe? SUSY is one of the most popular replacements for the common particle physics theories that lacks important features to explain mass hierarchy problem, how to unify fundamental forces of the Universe, dark matter, so on and so forth. MSSM is the collider friendly version of the SUSY and proposes some possible candidates for the dark matter along with solving the problems of SM naturally. In this thesis, two topological variables are examined in a specific SUSY decay, single lepton channel, by comparing their efficiencies in our analysis. These variables, W-stransverse mass and topness, are brand new and have been used seldom in previous analysis of CMS and ATLAS. It is highly expected that these variables will be more useful for the higher collision energies especially for the 14 TeV run of the LHC and 33 TeV run of the HL-LHC.

In the perspective of R-parity conserving MSSM, SUSY particles are produced in pairs and so it is expected to reconstruct an LSP pair originated from the mentioned decay channel. Single lepton channel, which is called the golden channel, is the main target of this research. We expect to see single lepton, multiple jets, at least two of which are b-tagged jets and two LSPs, which are undetected and taken into account as missing energy along with the neutrinos as final state particles. These final state particles are originated from the top squark pair produced as a result of the collision. By using the abovementioned special variables, we eliminate the background events and reconstruct the signal cascade decay in four STC scenarios for three possible

pile-up cases: 0, 50, and 140 pile-up. In this thesis, only the events with the first two families of leptons, i.e. e and μ types are used. τ leptons are not included and for the further researches, τ tagging might be used as well to increase number of possible signal scenarios and eliminate the background more efficiently. In addition, other decay channels such as fully hadronic and dileptonic would be analysed to obtain even more inclusive judgement for the difference between the dedicated variables.

After the control cuts, which are used almost all the SUSY analyses, we applied W-stransverve mass and topness variables interchangeably, and then compare the number of events left after both cases. As a result, we achieved an important improvement in the signal significance as it can be seen in the figures 4.39 , 4.39 , and 4.39. We observe a significant increase after applying the dedicated variables. However, there is no significant difference between the results of each. So, we can say that their efficiencies are almost the same. They can be used together or separately in the future analyses.

REFERENCES

[1] Paul Langacker. *The Standard Model and Beyond*. CRC Press, 2010.

[2] CMS Collaboration. Precise determination of the mass of the higgs boson and tests of compatibility of its couplings with the standard model predictions using proton collisions at 7 and 8 TeV. *The European Physical Journal C*, 75(5), 2015.

[3] CMS Collaboration and LHCb Collaboration. Observation of the rare $b_s^0 \to \mu^+\mu^-$ decay from the combined analysis of CMS and LHCB data. *Nature*, 522(7554):68–72, 06 2015.

[4] Combination of results on the rare decays $B_{(s)}^0 \to \mu^+\mu^-$ from the CMS and LHCB experiments. Technical Report CMS-PAS-BPH-13-007. CERN-LHCb-CONF-2013-012, CERN, Geneva, Jun 2014.

[5] Philip Bechtle, Tilman Plehn, and Christian Sander. Supersymmetry. In Thomas Schörner-Sadenius, editor, *The Large Hadron Collider*, pages 421–462. Springer International Publishing, 2015.

[6] Gautam Bhattacharyya. A pedagogical review of electroweak symmetry breaking scenarios. *Reports on Progress in Physics*, 74(2):026201, 2011.

[7] Planck Collaboration. Planck 2013 results. i. overview of products and scientific results. *A&A*, 571:A1, 2014.

[8] Gerard Jungman, Marc Kamionkowski, and Kim Griest. Supersymmetric dark matter. *Physics Reports*, 267(5–6):195 – 373, 1996.

[9] Richard J. Gaitskell. Direct detection of dark matter. *Annual Review of Nuclear and Particle Science*, 54(1):315–359, 2004.

[10] Steven Weinberg. A model of leptons. *Phys. Rev. Lett.*, 19:1264–1266, Nov 1967.

[11] Abdus Salam. Weak and Electromagnetic Interactions. *Conf. Proc.*, C680519:367–377, 1968.

[12] Sheldon L. Glashow. Partial-symmetries of weak interactions. *Nuclear Physics*, 22(4):579 – 588, 1961.

[13] Kien Nguyen. The higgs mechanism. `http://www.theorie.physik.uni-muenchen.de/lsfrey/teaching/archiv/sose_09/rng/higgs_mechanism.pdf`. Accessed: 2015-07-12.

[14] Jacek Dobaczewski. Non-linear σ model. http://www.fuw.edu.pl/~dobaczew/maub-42w/node12.html. Accessed: 2015-07-12.

[15] G.'t Hooft. Renormalization of massless yang-mills fields. *Nuclear Physics B*, 33(1):173 – 199, 1971.

[16] G.'t Hooft. Renormalizable lagrangians for massive yang-mills fields. *Nuclear Physics B*, 35(1):167 – 188, 1971.

[17] Patrick Labelle. *Supersymmetry demystified: a self teaching guide*. McGraw-Hill Education, 2009.

[18] 2001 CERN (European Organization for Nuclear Research). http://scienceblogs.com/startswithabang/2013/05/15/the-rise-and-fall-of-supersymmetry/ Accessed: 2015-07-12.

[19] J.-L. Gervais and B. Sakita. Generalizations of dual models. *Nuclear Physics B*, 34(2):477 – 492, 1971.

[20] Yu. A. Golfand and E. P. Likhtman. Extension of the Algebra of Poincare Group Generators and Violation of p Invariance. *JETP Lett.*, 13:323–326, 1971. [Pisma Zh. Eksp. Teor. Fiz.13,452(1971)].

[21] D.V. Volkov and V.P. Akulov. Is the neutrino a goldstone particle? *Physics Letters B*, 46(1):109 – 110, 1973.

[22] P. Fayet. Spontaneously broken supersymmetric theories of weak, electromagnetic and strong interactions. *Physics Letters B*, 69(4):489 – 494, 1977.

[23] Nir Polonsky. Supersymmetry: Structure and phenomena. Extensions of the standard model. *Lect. Notes Phys.*, M68:1–169, 2001.

[24] Gautam Bhattacharyya. Supersymmetry as a physics beyond the standard model. page 18, 2001.

[25] ATLAS Collaboration. Search for top squark pair production in final states with one isolated lepton, jets, and missing transverse momentum in s= 8 GeV pp collisions with the ATLAS detector. *Journal of High Energy Physics*, 2014(11), 2014.

[26] ATLAS Collaboration. Observation of a new particle in the search for the standard model higgs boson with the ATLAS detector at the LHC. *Physics Letters B*, 716(1):1 – 29, 2012.

[27] CMS Collaboration. Observation of a new boson at a mass of 125 GeV with the CMS experiment at the LHC. *Physics Letters B*, 716(1):30 – 61, 2012.

[28] John Ellis, Giovanni Ridolfi, and Fabio Zwirner. Radiative corrections to the masses of supersymmetric higgs bosons. *Physics Letters B*, 257(1–2):83 – 91, 1991.

[29] ATLAS Collaboration and CMS Collaboration. Combined measurement of the higgs boson mass in pp collisions at $\sqrt{s} = 7$ and 8 TeV with the ATLAS and CMS experiments.

[30] CMS Collaboration. Precise determination of the mass of the higgs boson and tests of compatibility of its couplings with the standard model predictions using proton collisions at 7 and 8 TeV. *The European Physical Journal C*, 75(5), 2015.

[31] Antoniadis, I. and Ghilencea, D. Supersymmetry after the higgs discovery. *Eur. Phys. J. C*, 74(5):2841, 2014.

[32] Experimental observation of isolated large transverse energy electrons with associated missing energy at s=540 GeV. *Physics Letters B*, 122(1):103 – 116, 1983.

[33] D. Guadagnoli and C. B. Park. MT2-reconstructed invisible momenta as spin analizers, and an application to top polarization. pages 298–316, 2011.

[34] C.G Lester and D.J Summers. Measuring masses of semi-invisibly decaying particle pairs produced at hadron colliders. *Physics Letters B*, 463(1):99 – 103, 1999.

[35] Hsin-Chia Cheng and Zhenyu Han. Minimal kinematic constraints and mt2. *Journal of High Energy Physics*, 2008(12):063, 2008.

[36] Search for supersymmetry in hadronic final states using MT2 with the CMS detector at $sqrt(s) = 8$ TeV. Technical Report CMS-PAS-SUS-13-019, CERN, Geneva, 2014.

[37] Yang Bai, Hsin-Chia Cheng, Jason Gallicchio, and Jiayin Gu. Stop the top background of the stop search. *Journal of High Energy Physics*, 2012(7), 2012.

[38] Michael L. Graesser and Jessie Shelton. Hunting mixed top squark decays. *Phys. Rev. Lett.*, 111:121802, Sep 2013.

[39] B.C. Allanach. Softsusy: A program for calculating supersymmetric spectra. *Computer Physics Communications*, 143(3):305 – 331, 2002.

[40] M. M. Mühlleitner, a. Djouadi, and M. Spira. Decays of supersymmetric particles - The program susy-hit. *Acta Physica Polonica B*, 38(2 PART 1):635–643, 2007.

[41] Johan Alwall, Michel Herquet, Fabio Maltoni, Olivier Mattelaer, and Tim Stelzer. Madgraph 5: going beyond. *Journal of High Energy Physics*, 2011(6), 2011.

[42] J. Alwall, R. Frederix, S. Frixione, V. Hirschi, F. Maltoni, O. Mattelaer, H.-S. Shao, T. Stelzer, P. Torrielli, and M. Zaro. The automated computation of tree-level and next-to-leading order differential cross sections, and their matching to parton shower simulations. *Journal of High Energy Physics*, 2014(7), 2014.

[43] Torbjörn Sjöstrand, Stephen Mrenna, and Peter Skands. Pythia 6.4 physics and manual. *Journal of High Energy Physics*, 2006(05):026, 2006.

[44] J. de Favereau, C. Delaere, P. Demin, A. Giammanco, V. Lemaître, A. Mertens, and M. Selvaggi. Delphes 3: a modular framework for fast simulation of a generic collider experiment. *Journal of High Energy Physics*, 2014(2), 2014.

[45] Florian Beaudette. The CMS Particle Flow Algorithm. In *Proceedings, International Conference on Calorimetry for the High Energy Frontier (CHEF 2013)*, pages 295–304, 2014.

[46] D. Krucker J. List A. Lobanov M. Berggren, A. Cakir and I.A. Melzer-Pellmann. Non-Simplified SUSY: stau-Coannihilation at LHC and ILC .

[47] CMS Collaboration. Search for supersymmetry in pp collisions at in events with a single lepton, large jet multiplicity, and multiple b jets. *Physics Letters B*, 733(0):328 – 353, 2014.

[48] ATLAS Collaboration. Measurement of the top quark pair production cross-section with ATLAS in the single lepton channel. *Physics Letters B*, 711(3–4):244 – 263, 2012.

[49] T.M.Liss and A.Quadt. The top quark. http://pdg.arsip.lipi.go.id/2013/reviews/rpp2012-rev-top-quark.pdf, last updated December 2011.

[50] CMS Collaboration. Search for top-squark pair production in the single-lepton final state in pp collisions at $\sqrt{s} = 8\ \mathrm{TeV}$. *The European Physical Journal C*, 73(12), 2013.

[51] Michael T. Meehan and Ian B. Whittingham. Dark matter relic density in gauss-bonnet braneworld cosmology. *Journal of Cosmology and Astroparticle Physics*, 2014(12):034, 2014.

[52] Kim Griest and David Seckel. Three exceptions in the calculation of relic abundances. *Phys. Rev. D*, 43:3191–3203, May 1991.

[53] M.Drees and G.Gerbier. Dark matter. http://pdg.lbl.gov/2013/reviews/rpp2013-rev-dark-matter.pdf.

[54] O. Buchmueller, R. Cavanaugh, A. De Roeck, J.R. Ellis, H. Flaecher, S. Heinemeyer, G. Isidori, K.A. Olive, F.J. Ronga, and G. Weiglein. Likelihood functions for supersymmetric observables in frequentist analyses of the cmssm and nuhm1. *The European Physical Journal C*, 64(3):391–415, 2009.

[55] Richard Arnowitt, Bhaskar Dutta, Teruki Kamon, Nikolay Kolev, and David Toback. Detection of SUSY in the stau–neutralino coannihilation region at the LHC. *Physics Letters B*, 639(1):46 – 53, 2006.

[56] DESY FLC Team. Desy flc physics studies: supersymmetry and wimp dark matter. http://www-flc.desy.de/ilcphysics/susy.php.

[57] Zachary Marshall and the Atlas Collaboration. Simulation of pile-up in the ATLAS experiment. *Journal of Physics: Conference Series*, 513(2):022024, 2014.

[58] Pippa Wells. Pileup mitigation at the HL-LHC. ECFA High Luminosity LHC Experiments Workshop - 2014, 2014.

[59] Stéphane Fartoukh. Pile up management at the high-luminosity LHC and introduction to the crab-kissing concept. *Phys. Rev. ST Accel. Beams*, 17:111001, Nov 2014.

[60] Supersymmetry discovery potential in future LHC and HL-LHC running with the CMS detector. Technical Report CMS-PAS-SUS-14-012, CERN, Geneva, 2015.

[61] Stephen H. Kan. *Metrics and Models in Software Quality Engineering*. Pearson Education, 2008.

[62] Glen Cowan and Eilam Gross. Discovery significance with statistical uncertainty in the background estimate. ATLAS Statistics Forum, 2008.

[63] Glen Cowan. Discovery sensitivity for a counting experiment with background uncertainty. 2012.

[64] ATLAS Collaboration. Measurement of the top quark pair production cross-section with ATLAS in the single lepton channel. *Physics Letters B*, 711(3–4):244 – 263, 2012.